RESEARCH ARTICLES

Resting-state functional connectivity predicts recovery from visually induced motion sickness

Jungo Miyazaki[1], Hiroki Yamamoto[2*], Yoshikatsu Ichimura[3], Hiroyuki Yamashiro[4], Tomokazu Murase[5], Tetsuya Yamamoto[6], Masahiro Umeda[7], Toshihiro Higuchi[5]

[1]Research and Development Department, Kyocera Corporation, Kanagawa, Japan
[2]Graduate School of Human and Environmental Studies, Kyoto University, Kyoto, Japan
[3]Corporate R&D, Canon Inc., Tokyo, Japan
[4]Department of Medical Engineering, Aino University, Osaka, Japan
[5]Departments of Neurosurgery, Meiji University of Oriental Medicine, Kyoto, Japan
[6]Department of System Neuroscience, National Institute for Physiological Sciences, Aichi, Japan
[7]Departments of Medical Informatics, Meiji University of Oriental Medicine, Kyoto, Japan

*Correspondence to: **Dr. Hiroki Yamamoto**
E-mail: yamamoto@cv.jinkan.kyoto-u.ac.jp
Tel: +81-75-753-2978; Fax: +81-75-753-6574
ORCID: 0000-0003-1051-6599

Keywords: motion sickness, fMRI, recovery, visual cortex, cingulate cortex, insula

Acknowledgements

This study was supported by Grants-in-Aid for Scientific Research on Innovative Areas “Shitsukan” (23135517, 25135720) from the Ministry of Education, Culture, Sports, Science and Technology of Japan and a Grant-in-Aid for Scientific Research (16K13506) from the Japan Society for the Promotion of Science (JSPS) to H. Yamamoto.

Abstract

Movies depicting certain types of motion often provoke uncomfortable symptoms similar to motion sickness, termed visually induced motion sickness (VIMS). VIMS generally evolves slowly during the viewing of a motion stimulus and, when the stimulus is removed, the recovery proceeds over time. Recent human neuroimaging studies have provided new insights into the neural bases of the evolution of VIMS. In contrast, no study has investigated the neural correlates of the recovery from VIMS. Study of the recovery process is critical for the development of a way to promote recovery and could provide further clues for understanding the mechanisms of VIMS. We thus investigated brain activity during the recovery from VIMS with functional connectivity magnetic resonance imaging. We found enhanced recovery-related functional connectivity patterns involving brain areas such as the insular, cingulate, and visual cortical regions, which have been suggested to play important roles in the emergence of VIMS. These regions also constituted large interactive networks. Furthermore, the increase in functional connectivity was correlated with the subjective awareness of recovery for the following five pairs of brain regions: insula–superior temporal gyrus, claustrum–left and right inferior parietal lobules, claustrum–superior temporal gyrus, and superior frontal gyrus–lentiform nucleus. Considering the previous findings on the functions of these regions and the present results, it is suggested that the increase in FC may reflect brain processes such as enhanced interoceptive awareness to one's own bodily state, a neuroplastic change in visual processing circuits, and/or the maintenance of visual spatial memory.

Introduction

First-person perspective images, such as movies captured by action cameras or drones, have recently become popular. Such movies are so realistic that viewers can feel as if they themselves are moving inside the image space. However, the rich image experience is associated with a side effect, termed visually induced motion sickness (VIMS), which involves unpleasant motion sickness (MS)-like symptoms caused by movies depicting certain types of movement. The symptoms are classified into three types: (1) oculomotor (eyestrain, difficulty focusing, headache), (2) nausea (stomach awareness, increased salivation, burping), and (3) disorientation (dizziness, vertigo, drowsiness) (Shupak & Gordon, 2006; Kennedy *et al.,* 2010). These symptoms can last for more than an hour (Kennedy *et al.,* 1993a; Ujike *et al.,* 2008).

VIMS generally emerges and evolves slowly during exposure to a motion stimulus, and, when the stimulus is removed, the individual slowly recovers from the MS symptoms over time. For the emergence and evolutional phase of VIMS, several neuroimaging studies have revealed the underlying brain response (Napadow *et al.,* 2013; Miyazaki *et al.,* 2015; Farmer *et al.,* 2015; Toschi *et al.,* 2017). Napadow *et al.* (2013) measured the functional magnetic resonance imaging (fMRI) activity of female participants during the presentation of translating black/white stripes for a long enough period to induce VIMS, finding that nausea was associated with a broad network of brain areas including the insula, cingulate cortex, and limbic regions, which are known to process stress, emotion, and interoception. In addition, Miyazaki *et al.* (2015) measured fMRI visual cortical activities during the evolutional phase of VIMS, which was provoked by the presentation of live-action images containing translational and rotational global motion components. The results showed that the activities of the middle temporal (MT+) area were desynchronised between the left and right hemispheres when participants had MS. The MT+ area has been suggested to interact with the parieto-insular vestibular cortex (PIVC), the centre of vestibular sensation, in the processing of self-motion stimuli that can induce VIMS (Brandt *et al.,* 1998; Kleinschmidt *et al.,* 2002; Smith *et al.,* 2012; Frank *et al.,* 2014, 2016). Taking these results together, the insular, cingulate, visual, vestibular cortical, and limbic regions are likely involved in the evolution of VIMS.

These findings seem to be consistent with several hypotheses concerning the incidence and evolution of MS. The modulation of the MT+ activities could be related to

the eye movement hypothesis (Ebenholtz, 1992; Ebenholtz *et al.,* 1994). This hypothesis proposes that exposure to a specific motion environment could induce abnormal eye movements that would stimulate the MS-related nuclei in the brainstem. The MT+ has been suggested to be intimately involved in eye movement control (Corbetta *et al.,* 1998; Dieterich *et al.,* 1998, 2003; Konen *et al.,* 2005) and therefore might also be associated with the incidence of MS. In addition, the involvement of PIVC may be related to the postural instability theory (Riccio & Stoffregen, 1991), indicating the importance of postural sway, which would be processed by the PIVC. Additionally, both visual and vestibular signals could be ascribed to the sensory conflict hypothesis (Reason & Brand, 1975; Reason, 1978; Oman, 1990), which proposes that mismatches between multiple sensory inputs such as visual and vestibular signals could lead to MS. Thus, recent neuroimaging studies have provided information on neural correlates of the emergence of VIMS in relation to its existing theories.

What happens during recovery from VIMS? Study of the recovery process from VIMS is critical for developing ways to promote recovery from the unpleasant symptoms of VIMS and could also provide clues for further investigation of its mechanisms. The brain processes related to the recovery phase of VIMS are still unclear but previous studies of unpleasant events similar to MS, such as fatigue or stress, may provide some hints. For example, Peltier *et al.* (2005) reported a fatigue-related reduction in functional connectivity, which was originally defined as a 'temporal correlation between spatially remote neurophysiological events' (Friston *et al.,* 1993), and functional connectivity has since been widely studied to elucidate functionally coordinated behaviour between brain regions. They measured fMRI time-series in the rest phase after participants completed a muscle fatigue task and found decreased functional connectivity between the motor cortices of the left and right hemispheres. In another example, van Marle *et al.* (2010) measured resting-state fMRI activity soon after female participants experienced psychological stress induced by viewing a strongly aversive movie. They reported increased functional coupling of the amygdala with the dorsal anterior cingulate cortex, anterior insula, and dorsorostral pontine region, indicating the extended state of hypervigilance that promotes sustained salience and mnemonic processing. These examples suggest that, during recovery, brain reorganisation could occur in functional brain networks related to the negative effects.

We therefore conjectured that such brain reorganisation would also occur during the recovery from VIMS. To test this prediction, we investigated resting-state fMRI activities during the recovery phase of VIMS. Specifically, we predicted that the functional connectivity of brain regions such as the insula, cingulate, visual, and/or vestibular cortical regions would be selectively changed because these regions have been linked to the emergence and evolutional phase of VIMS.

Methods

The present study analysed resting-state data obtained in our previous study (Miyazaki *et al.*, 2015), which provides details of the experiment and the task data.

Participants

Participants were 14 volunteers (12 men and 2 women, including 4 authors; mean age, 34.9 years; range, 25–48 years) with normal or corrected-to-normal vision. All participants had no history of neurologic or psychiatric disorder and provided written informed consent. All experimental procedures were approved by the Human Studies Committee of the Graduate School of Human and Environmental Studies at Kyoto University and the Department of Neurosurgery at Meiji University of Oriental Medicine.

Participants were classified into two groups: the VIMS group (n = 6, all men including 2 authors; mean age ± SD, 34.7 ± 8.0 years) who experienced VIMS in the experimental session; and the healthy group (n = 6, 2 women and 4 men including 2 authors; mean age ± SD, 33.3 ± 7.2 years) who did not experience VIMS. A possible concern is that the recruitment of some authors as participants would affect our results. We thus conducted three types of statistical analyses to address this possibility: a sub-analysis excluding the author participants, an analysis calculating the interclass correlation and design effect of authorship, and a linear mixed-effects model using authorship as one of the factors. None of the analyses suggested substantial effects of authorship.

The VIMS or healthy classification was performed using a self-reported VIMS (yes or no) by asking, ‘Did you get motion sick during the experimental session?’. Two of the participants in the VIMS group were subsequently excluded from the analysis of the recovery process because they had not recovered from the VIMS according to the Simulator Sickness Questionnaire (SSQ) score (Kennedy *et al.*, 1993b). Briefly, the SSQ

was developed as a standard measure for evaluating the severity of simulator sickness and has also been used to measure VIMS symptoms. However, several studies (Stanney *et al.*, 1998; Stoffregen *et al.*, 2019; Walter *et al.*, 2019) have indicated that the SSQ could deviate from self-reports. Such a discrepancy was not observed in the present study. The SSQ scores of the VIMS group markedly increased immediately after the VIMS-inducing stimulus and decreased to a normal level during the subsequent rest (recovery) phase (except for the abovementioned 2 participants), whereas the SSQ scores of the healthy group did not change throughout the experimental session (see Figure 4 in Miyazaki *et al.* [2015]), suggesting that the SSQ scores show a similar trend to the self-reports.

Visual stimuli

In the experiment, two types of visual stimuli—a global motion stimulus and a local one—were presented. The global motion stimulus was a 6-min-long live-action movie containing first-person-perspective, global visual motion. This stimulus content could induce VIMS in viewers. In contrast, the local motion stimulus was a 6-min-long live-action movie consisting of 8 by 8 patches (total, 64), which reduced the global motion stimulus to one-eighth vertically and horizontally. This stimulus was a control and did not induce VIMS in viewers because the stimulus contained no global motion component that could trigger VIMS. The stimulus was based on Wall and Smith (2008).

These stimuli were projected onto a screen located over the participant's forehead using a DLP projector (LVP-HC3800; Mitsubishi, Japan). The spatial resolution was 1080 × 720 pixels, and the refresh rate was 60 Hz. The participant was supine and viewed the stimuli through a planar mirror located 25 cm from the eyes. See Miyazaki *et al.* (2015) for details.

Experimental procedure

The experimental procedure is shown in Figure 1. Before and after the presentation of the two aforementioned stimuli, three rest phases (Rest-1, Rest-2, and Rest-3) were arranged. Each rest phase was 5 min long and comprised presentation of a grey background with a fixation point at the centre. Before the experimental session, participants were instructed to relax with their eyes open during the rest phases, and participants were allowed to leave the experiment at any time if they could not continue the session. Throughout the session,

participants lay supine on the MRI scanner table without firm restriction of their head or body so as to minimise undesired effects such as pain and distraction. After the first rest phase (Rest-1), participants viewed the local motion stimulus; none experienced VIMS. Next, the participants experienced the second rest phase (Rest-2) and then viewed the global motion stimulus; 8 of the 14 participants experienced VIMS, as described above. The third rest phase (Rest-3) followed. The order of the stimulus presentations (the local motion stimulus followed by the global one) was not balanced to avoid a carryover effect from the global to the local motion period because our preliminary experiment had indicated that, when the global stimulus precedes the local one, the VIMS symptoms can be prolonged and overlap the subsequent local stimulus presentation.

To rate the degree of VIMS symptoms, participants answered the Simulator Sickness Questionnaire (SSQ) (Kennedy *et al.*, 1993b) 6 times in total, that is, before and after each stimulus presentation and each rest phase. The SSQ was developed as a metric of simulator sickness, and this metric consists of 16 questions on symptoms such as headache and nausea, based on four grades. The SSQ has generally also been used as a metric for VIMS. The question items of the SSQ were presented to participants through images, and the questions were answered by use of a response pad with four buttons (HH-1x4L; Current Design Inc., Philadelphia, PA). A decrease in the SSQ scores between before and after the rest phases, which would reflect recovery from VIMS, was analysed because the aim of the present study was to investigate the recovery phase of VIMS at rest.

(Please place Figure 1 around here)

MRI data acquisition

Functional MR images were acquired using a clinical 3-T MR scanner (Trio TIM; Siemens, Germany) and a 20-channel phased-array head coil with a $T2^*$-weighted gradient-echo echo planar sequence (repetition time [TR] = 2000 ms; echo time [TE] = 30 ms; flip angle [FA] = 90°; voxel size [VS] = 3 mm × 3 mm × 4 mm; field of view [FOV] = 192 mm × 192 mm; 37 slices; axial orientation parallel to the AC-PC plane; interleaved acquisition). The functional images were continuously scanned from 10 s before Rest-1 to the end of Rest-3, taking about 35 min. For anatomical registration, brain

structural images were acquired using a 3D magnetisation-prepared rapid gradient-echo T1-weighted sequence with the following parameters: TR = 1800 ms, TE = 3.03 ms, inversion time = 650 ms, FA = 9°, VS = 0.8 mm × 0.8 mm × 0.8 mm, FOV = 205 mm × 205 mm, 176 slices, axial orientation parallel to the AC-PC plane, interleaved acquisition.

Behavioural data analyses

Visually induced motion sickness

After the experimental session, participants self-reported whether or not they experienced VIMS while viewing the global motion stimulus and were provisionally classified into the VIMS or healthy group based on the self-report as mentioned above. To objectively test the validity of this grouping criterion based on the self-reports, SSQ scores, which are a metric for MS symptoms, were statistically tested to determine whether the scores of the VIMS group selectively increased after the global motion stimulus. Details of this analysis are provided in Miyazaki *et al.* (2015).

Recovery from visually induced motion sickness

Next, to verify that the VIMS group participants recovered during Rest-3, the differences in the SSQ scores between before and after each rest phase were computed, and the differences were statistically tested to determine whether the score of the VIMS group became significantly larger only for Rest-3, reflecting the recovery from VIMS, and whether the scores of the other rest phases did not change. To facilitate interpretation of the results, we examined not only the SSQ Total Score, but also the other three subscales: Oculomotor, Nausea, and Disorientation. This analysis was performed using R software (R Core Team, 2017) (see also Miyazaki *et al.,* 2015). A linear mixed-effects model analysis was performed with the *lmer* function of the lme4 package (Bates *et al.,* 2014). This model had a within-participants fixed effect PHASE (Rest-1 *vs.* Rest-2 *vs.* Rest-3), a between-participants fixed effect GROUP (VIMS *vs.* healthy participant groups), an interaction of PHASE and GROUP, and a random effect of each individual participant. This analysis was conducted separately for the four scales of the SSQ (Total Score, Nausea, Oculomotor, and Disorientation).

When the PHASE × GROUP interaction was statistically significant, for the *post hoc* analysis, the simple effect of PHASE was tested separately for the VIMS and healthy

groups. Specifically, the differences in scores between the levels of PHASE (i.e., three ways of Rest-1 *vs.* Rest-2; Rest-2 *vs.* Rest-3; and Rest-1 *vs.* Rest-3) were tested by means of the functions *testInteractions* and *testFactors* of the phia package (De Rosario-Martinez, 2015) separately for each participant's group. In contrast, when the interaction was not significant, the main effect of PHASE was reported instead. The significance level for all statistical analyses was set to 0.05, with correction by the Bonferroni method for multiple comparisons involving the four scales of the SSQ, the two participant groups, and the repetition of the *post hoc* tests.

fMRI data analyses

Preprocessing

All fMRI data were preprocessed using AFNI software (Cox, 1996) as follows: (1) slice timing correction; (2) head motion correction; (3) extraction of 5-min-long time-series signals (150 fMRI volumes) acquired during each rest phase; (4) transformation to the standard Talairach space for group analysis; (5) smoothing with the Gaussian kernel of an isotropic 9-mm FWHM; (6) band-pass filtering with a cutoff of 0.01–0.1 Hz; and (7) removal of fMRI volumes whose motion or its derivatives exceeded 0.2 mm (i.e., motion 'scrubbing') to reduce the effect of head movement on fMRI data, in addition to the removal of outlier volumes where the ratio of the number of outlier voxels exceeded 0.1.

Brain connectedness mapping

After the preprocessing, connectedness maps were made by use of the AFNI *3dTcorrMap* function. Connectedness is the average of the Pearson correlation coefficients between a specific voxel time-series and the other in the brain mask (Gotts *et al.*, 2012). The Pearson correlation coefficient is a real number ranging from –1 to +1, and this value was converted to a Fisher's *Z* value with the *3dTCorrMap* function for the following analyses. The Z values were compared between the VIMS and healthy groups within the Talairach space by using the AFNI *3dLME* function. For the mapping of the results of this comparison, the voxel-wise *P* value was set to 0.0001. The false-positive rate for the clustering was estimated by use of the *3dClustSim* function, in which the threshold α for the cluster size was set to 0.10; this relatively loose threshold was used because this was a first screening procedure to restrict candidates. The conventional 0.05 threshold was

used in the second screening based on functional connectivity described below. Based on this mapping, the regions whose connectedness changed significantly during the recovery phase of VIMS were detected. Specifically, the regions were determined according to the following criteria: the connectedness was changed only for the VIMS group selectively during Rest-3 when the VIMS participants experienced VIMS, whereas that of the healthy group did not change for all rest phases (interaction contrast calculated using the *3dLME* function: absolute intergroup difference in $Z_{Rest\text{-}3} - 0.5 \times Z_{Rest\text{-}1} - 0.5 \times Z_{Rest\text{-}2}$: the VIMS group – the healthy group > 3.891, which corresponds to $P < 0.0001$).

Through these steps, 12 brain regions were identified with significant changes in connectedness during recovery from VIMS (described below). In each region, the mean time-series averaged across voxels within the region was calculated and used as a seed for the functional connectivity analysis in the following section.

ROI-based functional connectivity analysis

As stated above, the mean time-series averaged across voxels within the brain regions showing significant changes in connectedness during recovery from VIMS were used as seeds to examine functional connectivity throughout the entire brain. Then, using the same method as in the analysis of connectedness, functional connectivity intensity was compared between the VIMS and healthy groups. After adjustment to the false-positive rate for clustering, the result was mapped in Talairach space (voxel-wise *P* value = 0.0001, $\alpha = 0.05$), through which the brain regions with changes in functional connectivity during recovery from VIMS that fulfilled the following criteria were identified: (i) functional connectivity in Rest-3 following the onset of VIMS changed only in the VIMS group (interaction contrast calculated using the *3dLME* function: absolute intergroup difference in $Z_{Rest\text{-}3} - 0.5 \times Z_{Rest\text{-}1} - 0.5 \times Z_{Rest\text{-}2}$: the VIMS group–the healthy group > 3.891, which corresponds to $P < 0.0001$) and (ii) neither group had a change in functional connectivity during other rest phases (the VIMS group, $|Z_{Rest\text{-}2} - Z_{Rest\text{-}1}| < 1.96$, which corresponds to $P > 0.05$; the healthy group, $|Z_{Rest\text{-}3} - 0.5 \times Z_{Rest\text{-}1} - 0.5 \times Z_{Rest\text{-}2}| < 1.96$; $|Z_{Rest\text{-}2} - Z_{Rest\text{-}1}| < 1.96$).

This functional connectivity analysis extracted 19 pairs of brain regions, and changes in each functional connectivity were analysed using R software (R Core Team, 2017) and a linear mixed-effects model (the same model used in the analysis of the SSQ scores)

consisting of a within-participants fixed effect (PHASE; Rest-1 *vs.* Rest-2 *vs.* Rest-3), a between-participants fixed effect (GROUP; VIMS *vs.* the healthy group), an interaction of PHASE and GROUP, and a random effect of each individual participant.

Because the PHASE × GROUP interactions for all region pairs were statistically significant, a *post hoc* test was performed to analyse the simple main effect of PHASE in the VIMS and healthy groups separately. Specifically, the differences in connectivity between Rest-1 and Rest-2, Rest-2 and Rest-3, and Rest-1 and Rest-3 were tested in each group. The Bonferroni method was used to correct multiple comparisons for functional connectivities in the 19 pairs of brain regions, the two participant groups, and repeated *post hoc* tests of the three PHASE combinations.

Correlation analysis

Correlation analysis was performed to clarify whether a change in the SSQ Total Score (i.e., subjective awareness of recovery) could be predicted from the change in functional connectivity. Because exceptionally large changes in SSQ Total Scores were observed in some participants, the Spearman's rank correlation coefficient, a nonparametric statistic that is seldom affected by such variation, was used to analyse the 19 pairs of brain regions separately. Because of the multiple comparisons, *P* values were subjected to Bonferroni correction.

Global network analyses

To analyse the functional network of the brain regions showing recovery-related increases in connectedness, a multivariate analysis was performed. First, for each participant and for each rest phase, a partial correlation coefficient of the fMRI time-series was computed for each pair of the 12 brain regions, resulting in a 12 × 12 matrix. The partial correlation matrix was then converted into a distance matrix, where the distance was defined by 1 minus the absolute partial correlation coefficient. Second, for each rest phase, within-group averaged distance matrices were computed for VIMS and healthy groups. The distance matrices of the first phase (Rest-1) and second phase (Rest-2) were further averaged as a control for the recovery phase (Rest-3). Third, the columns and rows of the distance matrices were reordered to place similar brain regions closer, using the *seriation* function with the 'HC' option in the *seriation* package (Hahsler *et al.*, 2008) of R software.

Finally, dendrograms, which are hierarchical clustering trees, were derived from the distance matrices using the *pvclust* package (Suzuki & Shimodaira, 2019) of R software, which provided *P* values of each cluster through multiscale bootstrap resampling. Independently of the above analyses, statistically independent brain networks were extracted by a dictionary learning framework. The procedure and the results are detailed in the Supplementary Materials.

Results

Behavioural results

Details of the results for VIMS symptoms induced in the experiment are provided in Miyazaki *et al.* (2015). In brief, 8 of the 14 participants experienced VIMS due to the global motion stimulus, and the remaining 6 did not (Figs. 3 and 4 of Miyazaki *et al.* [2015]). These results were confirmed by statistical analysis of the SSQ scores (Table 1 of Miyazaki *et al.* [2015]). Participants were divided into VIMS (n = 8) and healthy (n = 6) groups based on the presence and absence of VIMS, respectively. However, 2 of the 8 participants in the VIMS group did not recover from the VIMS even after the experimental session, and this was reflected in their SSQ scores, which did not decrease even after Rest-3. Because the aim of this study was to analyse the recovery phase of VIMS, these 2 participants were excluded from the subsequent analyses.

To verify that the participants in the VIMS group had recovered from VIMS during Rest-3, a linear mixed-effects model analysis of the SSQ score was performed before and after each rest phase (Table 1 and Fig. 2). SSQ Total Scores decreased during Rest-3 only in the VIMS group. The interaction of PHASE and GROUP was statistically significant ($\chi^2(2) = 13.30$, $P = 0.005$, Bonferroni corrected). A *post hoc* test of the simple main effect of PHASE showed that SSQ scores decreased significantly during Rest-3 only in the VIMS group (the VIMS group: Rest-1 *vs.* Rest-2: $\chi^2(2) = 0.03$, $P > 1$; Rest-2 *vs.* Rest-3: $\chi^2(2) = 15.04$, $P = 0.001$; Rest-1 *vs.* Rest-3: $\chi^2(2) = 16.41$, $P = 0.0007$; the healthy group: Rest-1 *vs.* Rest-2: $\chi^2(2) = 4.72$, $P = 0.417$; Rest-2 *vs.* Rest-3: $\chi^2(2) = 0.07$, $P > 1$; Rest-1 *vs.* Rest-3: $\chi^2(2) = 5.98$, $P = 0.203$, Bonferroni corrected), verifying that the participants in the VIMS group recovered from the VIMS during Rest-3.

Among the three SSQ subscales, the Disorientation score was similar to the Total Score (PHASE × GROUP interaction: $\chi^2(2) = 19.16$, $P = 0.0002$; *post hoc* test: the VIMS

group: Rest-1 *vs.* Rest-2: $\chi^2(2) = 0.02$, $P > 1$; Rest-2 *vs.* Rest-3: $\chi^2(2) = 18.52$, $P = 0.0002$; Rest-1 *vs.* Rest-3: $\chi^2(2) = 19.87$, $P = 0.0001$; the healthy group: Rest-1 *vs.* Rest-2: $\chi^2(2) = 0.53$, $P > 1$; Rest-2 *vs.* Rest-3: $\chi^2(2) < 0.01$, $P > 1$; Rest-1 *vs.* Rest-3: $\chi^2(2) = 0.52$, $P > 1$, Bonferroni corrected). As for Nausea and Oculomotor, the PHASE × GROUP interactions were not significant (Nausea, $\chi^2(2) = 7.74$, $P = 0.084$; Oculomotor, $\chi^2(2) = 5.48$, $P = 0.259$; Bonferroni corrected), and the main effect of PHASE was also not significant (Nausea, $\chi^2(2) = 4.28$, $P = 0.539$; Oculomotor, $\chi^2(2) = 4.62$, $P = 0.444$; Bonferroni corrected).

(Please place Figure 2 and Table 1 around here)

Brain connectedness mapping

To test our hypothesis that the recovery phase of VIMS induces changes in functional connectivity in some brain regions, we examined the substantial changes in functional connectivity by calculating connectedness, which is the mean correlation coefficient of a specific voxel time-series to other voxel time-series (Gotts *et al.*, 2012), and then by mapping the results in Talairach space. As anticipated, the map revealed 12 brain regions with significant increases in connectedness during Rest-3 in the VIMS group (Table 2 and Fig. 3). The 12 regions included the primary visual cortex in the occipital cortex (the left and right lingual gyrus; Fig. 3k and g, respectively) and the left and right insula (Fig. 3c and d) and cingulate regions (the right anterior cingulate and left cingulate gyrus; Fig. 3b and h, respectively). In addition, the left superior frontal gyrus (Fig. 3j) and the right inferior frontal gyrus (Fig. 3l) were included in the 12 brain regions. Furthermore, connectedness significantly increased in the cerebellum (left cerebellar tonsil; Fig. 3e) and the subcortical region (left and right thalamus and the right claustrum; Fig. 3a, i, and f, respectively) during the recovery phase of VIMS. In contrast, no brain region had a significant decrease in connectedness during the recovery phase.

(Please place Figure 3 and Table 2 around here)

ROI-based functional connectivity analyses

For the 12 ROIs with increased connectedness, the question arose as to whether functional

connectivity had increased in a broad area or in only specific regions. To address this question, the entire brain was screened for functional connectivity using the 12 ROIs as seeds. It was found that 8 of the 12 seed regions showed increases in functional connectivity with specific regions during only Rest-3 (recovery phase) for the VIMS group. These regions were the left thalamus, left and right insula, left cerebellar tonsil, right claustrum, left cingulate gyrus, left superior frontal gyrus, and left inferior frontal gyrus. Each of these regions had selective increases in functional connectivity with several other regions, resulting in the following 19 region pairs: left thalamus–right insula, left thalamus–right inferior parietal lobule, left thalamus–right declive, left insula–left thalamus, left insula–left inferior parietal lobule, right insula–left superior temporal gyrus, right insula–left inferior temporal gyrus, left cerebellar tonsil–left parahippocampal gyrus, right claustrum–left cingulate gyrus, right claustrum–right inferior parietal lobule, right claustrum–left inferior frontal gyrus, right claustrum–left superior temporal gyrus, right claustrum–left inferior parietal lobule, left cingulate gyrus–right insula, left superior frontal gyrus–left medial frontal gyrus, left superior frontal gyrus–left middle temporal gyrus, left superior frontal gyrus–left lentiform nucleus, and right inferior frontal gyrus–left inferior frontal gyrus (Table 3). The locations of the 19 pairs are shown in the left panels of Figure 4 and Supplementary Figure 1. The other 4 of the 12 seed regions had no selective changes in functional connectivity.

The phase (Rest-1, -2, and -3) × group (Healthy and VIMS) interaction effect can be clearly seen in the right panels of Figure 4 and Supplementary Figure 1. The functional connectivity of the VIMS group (yellow solid line) remained comparable in Rest-1 and Rest-2 but increased in Rest-3 (recovery phase), whereas that of the healthy group (white broken line) did not show an increase in any phase. These results were statistically confirmed by a linear mixed-effects model analysis. The interaction effects of resting phases (PHASE: Rest-1, Rest-2, and Rest-3) and participants' group (GROUP: VIMS and healthy) were statistically significant for all 19 pairs (Table 3). We thus analysed the simple effect of PHASE separately for the VIMS and healthy groups. The statistical results for the VIMS and healthy groups are shown in Tables 4 and 5, respectively. The selective increases in functional connectivity for the VIMS group during Rest-3 (recovery phase) were statistically significant for almost all pairs and the effect sizes (Cohen's *d*) were relatively large (Table 4). For example, for the right insula–left thalamus pair (#6 in

Tables 4 and 5), the simple effect of the Rest-3 PHASE was statistically significant for only the VIMS group (Rest-2 *vs.* Rest-3: $\chi^2(2) = 53.99$, $P = 2 \times 10^{-11}$, Cohen's $d = 3.00$; Rest-1 *vs.* Rest-3: $\chi^2(2) = 38.05$, $P = 8 \times 10^{-8}$, Cohen's $d = 2.52$, Bonferroni corrected) (#6 in Table 4), whereas this effect was not found for the other control conditions (VIMS group: Rest-1 *vs.* Rest-2: $\chi^2(2) = 1.39$, $P > 1$, Cohen's $d = 0.48$; healthy group: Rest-1 *vs.* Rest-2: $\chi^2(2) = 0.13$, $P > 1$, Cohen's $d = 0.15$; Rest-2 *vs.* Rest-3: $\chi^2(2) = 0.88$, $P > 1$, Cohen's $d = 0.38$; Rest-1 *vs.* Rest-3: $\chi^2(2) = 1.70$, $P > 1$, Cohen's $d = 0.53$, Bonferroni corrected) (#6 in Tables 4 and 5). Similar selective changes in functional connectivity were observed in the other 18 region pairs (see Tables 3, 4, and 5). However, as an exception, the functional connectivity between the left superior frontal gyrus and left middle temporal gyrus showed a tendency toward an increase in the second *vs.* third rest phases in the VIMS group (#17 in Table 4).

(Please place Figure 4 and Tables 3, 4, and 5 around here)

Correlation analyses

To determine whether the increases in functional connectivity were associated with subjective recovery from VIMS, we conducted correlation analyses between the change in functional connectivity and that in the SSQ Total Scores for the 19 pairs of brain regions (Fig. 5). The following 5 pairs showed statistically significant negative correlations, indicating regions in which greater increases in functional connectivity were associated with greater recovery from VIMS: the right insula–left superior temporal gyrus (Spearman's rank correlation $\rho = -0.83$, $P = 0.017$, Fig. 5a), right claustrum–right inferior parietal lobule ($\rho = -0.83$, $P = 0.016$, Fig. 5b), right claustrum–left superior temporal gyrus ($\rho = -0.92$, $P = 0.0004$, Fig. 5c), right claustrum–left inferior parietal lobule ($\rho = -0.80$, $P = 0.038$, Fig. 5d), and left superior frontal gyrus–left lentiform nucleus ($\rho = -0.80$, $P = 0.038$, Fig. 5e; all Bonferroni corrected). The correlation was not statistically significant in the remaining 14 pairs: the left thalamus–right insula ($\rho = -0.64$, $P = 0.469$), left thalamus–right inferior parietal lobule ($\rho = -0.63$, $P = 0.510$), left thalamus–right declive ($\rho = -0.71$, $P = 0.181$), left insula–left thalamus ($\rho = -0.73$, $P = 0.137$), left insula–left inferior parietal lobule ($\rho = -0.62$, $P = 0.576$), right insula–left thalamus ($\rho = -0.67$, $P = 0.330$), right insula–left inferior temporal gyrus ($\rho = -0.61$, $P = 0.647$), left cerebellar

tonsil–left parahippocampal gyrus (ρ = −0.71, *P* = 0.181), right claustrum–left cingulate gyrus (ρ = −0.75, *P* = 0.095), right claustrum–left inferior frontal gyrus (ρ = −0.74, *P* = 0.115), left cingulate gyrus–right insula (ρ = −0.70, *P* = 0.212), left superior frontal gyrus–left medial frontal gyrus (ρ = −0.63, *P* = 0.510), left superior frontal gyrus–left middle temporal gyrus (ρ = −0.58, *P* = 0.932), and right inferior frontal gyrus–left inferior frontal gyrus (ρ = −0.61, *P* = 0.698; all Bonferroni corrected).

(Please place Figure 5 around here)

Global network analyses

The above connectedness map shows the 12 brain regions with recovery-selective increases in connectedness (Fig. 3 and Table 2). To explore the possibility that these regions constituted larger functional networks, we conducted a multivariate analysis in which the network of these regions was analysed based on distance matrices representing dissimilarity among the fMRI time-series in each pair of these regions (Supplementary Figure 2), from which hierarchical clustering dendrograms were derived. Figure 6 compares the results of the VIMS group (a, c) with those of the healthy group (b, d). As clearly shown in Fig. 6, the 12 brain regions of the VIMS group showed more global network structures for both recovery (Rest-3) and non-recovery (the average of Rest-1 and Rest-2) phases, in contrast to the healthy group, for which there was only a statistically significant cluster (marked with asterisks) of the left and right lingual gyri. Notably, the statistically significant clusters of the VIMS group (marked with asterisks) comprised the brain regions with recovery-selective increases in ROI-based functional connectivity (marked with underlines) and the regions with correlation with the SSQ (marked with italics), corroborating the above analyses (Figs. 4 and 5). During the recovery phase (Rest-3), the left thalamus additionally participated in the visual cortical cluster, and this cluster was combined with the other cluster of the left/right insular and cingulate areas in a higher level. Interestingly, during the phases before sickness developed, the VIMS group already showed a distinct cluster composed of the left cingulate gyrus and right thalamus in conjunction with the visual cortical cluster. Some of these networks were also independently confirmed by dictionary learning-based

connectivity mapping (Supplementary Figure 3).

(Please place Figure 6 around here)

Discussion

Here, we investigated resting-state fMRI functional connectivity during the recovery phase of VIMS. The analysis showed increased functional connectivity in some brain areas, including the insula, cingulate, and visual cortical regions. These regions were also found to constitute large interactive networks. Furthermore, some of the connectivity increases were strongly correlated with the subjective awareness of recovery from VIMS (decrease in subjective SSQ scores) for the following five pairs of brain regions: the insula–superior temporal gyrus, claustrum–left inferior parietal lobule, claustrum–right inferior parietal lobule, claustrum–superior temporal gyrus, and superior frontal gyrus–lentiform nucleus. These brain regions included key areas related to the emergence and evolution of VIMS. The insula had increased connectivity with the cingulate gyrus during recovery from VIMS (Supplementary Figure 1k). The insular and cingulate regions have also exhibited a correlated activation during a higher nausea state (Napadow *et al.*, 2013). Additionally, the insula showed a significant correlation between sympathovagal balance and connectivity with a middle temporal region (MT+/V5) during a visually induced nausea sensation (Toschi *et al.*, 2017), which is a visual motion-sensitive area. Moreover, the middle temporal region has exhibited decreased inter-hemispheric synchronisation during VIMS (Miyazaki *et al.*, 2015). Here, this key area had increased connectivity with the superior frontal region during recovery from VIMS (Supplementary Figure 1m). In addition to these key brain areas, several regions detected in our analysis of the recovery from VIMS, such as the inferior frontal gyrus (Supplementary Figure 1j and 1n), cerebellar tonsil (Supplementary Figure 1h), and declive (Supplementary Figure 1c), have been linked to the evolution of VIMS (Farmer *et al.*, 2015). These results thus conformed with our initial expectations that key brain regions related to the emergence and evolution of VIMS could also be involved in the recovery. Further studies are required to verify this speculation because the present work is a correlational study that cannot establish a causal relationship.

In our experiment, the 2 female participants did not experience motion sick and were

included in the healthy group. This result is somewhat inconsistent with the view that women are more susceptible to MS than men (Munafo *et al.,* 2017). This may be simply due to the small sample size and/or the difference in experimental stimuli. The type of visual motion stimuli has been reported to affect the sex difference in MS incidence: the translational motion stimulus induced a sex difference in MS incidence, whereas the rotational one did not (Klosterhalfen *et al.,* 2006; Koslucher *et al.,* 2015; Munafo *et al.,* 2017). It thus seems that our global motion stimulus, which included a rotational component caused by camera rotation, might have difficulty inducing a sex difference.

A closer look at the changes in functional connectivity along the resting phases (Rest-1, Rest-2, and Rest-3) (Fig. 4) suggests two different groups that might have distinct roles among the five pairs of brain regions. For the first group, the right insula–superior temporal gyrus (Fig. 4a) and the superior frontal gyrus–lentiform nucleus (Fig. 4e), functional connectivity remained roughly comparable in the healthy and VIMS groups before the VIMS (Rest-1 and Rest-2) but increased only in the VIMS group during the recovery from VIMS (Rest-3), indicating temporary reorganisations of neural circuitry triggered by the experience of unusual motion environments. In contrast, for the second group, the claustrum–inferior parietal lobule (Fig. 4b and 4d), functional connectivity was weaker in the VIMS group than in the healthy group before the onset of VIMS but became comparable in the two groups during the recovery from VIMS. A similar intrinsic difference between the groups was also observed in the dendrogram (Fig. 6c vs. Fig. 6d). These results imply that VIMS group participants might have weaker connectivities between specific brain regions, possibly reflecting VMIS susceptibility and/or tolerance. It would be interesting to address MS susceptibility and/or tolerance in a future study with a larger sample size.

The main limitations of this study include its small sample size and its correlational nature. However, this is the first study to elucidate the brain process in the recovery phase of VIMS. Thus, it would be interesting to discuss possible reasons why the functional connectivity between the brain regions increased during the recovery from VIMS. Here, we propose three possibilities and discuss them in relation to the current understanding of VIMS and related hypotheses. The first possibility is that the changes in functional connectivity observed during the recovery phase could be related to interoceptive awareness (perception of one's own bodily state) because interoceptive awareness is

expected to increase to alleviate the symptoms of VIMS, such as dizziness, eye pain, and nausea. In this regard, it is interesting that connectivities, including those of insular and cingulate regions, were increased in our study. The insular cortex, the likely centre of the neural basis of interoception, is also regarded as the limbic sensory cortex (Craig, 2002; Craig & Craig, 2009) because this brain site might be involved in the homeostatic regulation of the brain stem. In addition, the cingulate gyrus is also known as the limbic motor cortex and might contribute to interoception together with the insular cortex (Craig, 2002; Craig & Craig, 2009). Indeed, according to Napadow *et al.* (2013), the cingulate cortex is coactivated with the insular cortex when the perception of nausea is triggered by visual stimuli. The claustrum, which had functional connectivity with multiple brain regions in this study, has been reported to be involved in the processing of conscious perception, suggesting its association with interoceptive perception (Crick & Koch, 2005). Therefore, the strengthened brain networks centring on the insula and claustrum in this study might reflect the internal perception of a poor physical state triggered by VIMS. Similarly, after observing the strengthening of the amygdala network (including the insular cortex) immediately after the induction of psychological stress by visual stimuli, van Marle *et al.* (2009) suggested that the strengthened amygdala network might reflect negative hypervigilance.

The second possibility is that the changes in functional connectivity observed during the recovery phase of VIMS could reflect plastic changes in neural circuits related to visual processing, such as visual attention and eye movement control. In this regard, we note that visual processing regions, including the middle temporal gyrus, which is a visual motion-sensitive area, exhibited significantly increased functional connectivity during the recovery phase of VIMS in our study. Indeed, the middle temporal gyrus had strong connectivity with the superior frontal gyrus (Supplementary Figure 1m and #17 in Tables 3, 4, and 5). Interestingly, similar results were reported in previous neuroimaging studies of visual or motor learning (Albert *et al.*, 2009a, b; Lewis *et al.*, 2009; Stevens *et al.*, 2009, 2015). Stevens *et al.* (2009) showed that functional connectivities between the neural network in the occipital face and scene areas and frontal cortex were increased during the rest phase immediately after a visual face and scene recognition task and that subsequent memory retrieval performance was predicted by the extent of the changes in the functional connectivity. This suggests that a functional connectivity increase during a

rest phase after a task might reflect the neuroplastic change needed to improve the efficacy of task processing. In addition to this change in connectivity between occipital visual and frontal regions, brain areas showing increased functional connectivity in this study (the insula–superior temporal gyrus [Figure 4A], insula–inferior temporal gyrus [Supplementary Figure 1g], cingulate gyrus–insula [Supplementary Figure 1k], superior frontal gyrus–medial frontal gyrus [Supplementary Figure 1l], and left and right inferior frontal gyrus [Supplementary Figure 1n]) were coactivated when regulating visual attention or eye movement in previous fMRI studies (Corbetta *et al.*, 1998; Dieterich *et al.*, 1998, 2003; Konen *et al.*, 2005). As for the increased connectivity of the claustrum to multiple brain regions in this study, this area is related to visual and multisensory attention and was reported to be activated at the same time as the inferior parietal lobule and interior frontal gyrus (Vohn *et al.*, 2007), both of which were detected in this study. Attention is closely associated with eye movement (Corbetta *et al.*, 1998), and eye movement has been proposed to cause MS, including VIMS, in the eye movement hypothesis (Ebenholtz, 1992; Ebenholtz *et al.*, 1994). The eye movement hypothesis posits that MS is caused by abnormal eye movement induced in a certain type of motion environment. Given this prior knowledge and our results, the increase in functional connectivity observed during the recovery from VIMS might reflect a plastic change in neural circuits related to visual processing, such as visual attention and/or eye movement control.

Another putative neuronal circuit of VIMS is the vestibular cortex, which is concerned with balance sensation. Previous neuroimaging studies employing visual and vestibular stimuli suggested a close cooperation between the motion-sensitive visual cortices and vestibular cortex for self-motion perception (Brandt *et al.*, 1998; Kleinschmidt *et al.*, 2002; Smith *et al.*, 2012; Frank *et al.*, 2014, 2016). In addition, we observed significant changes in functional connectivity in the higher-order visual areas of the inferior and middle temporal gyri during recovery from VIMS (Supplementary Figure 1g and 1m; Tables 3, 4, and 5). However, no change in connectivity was seen in the PIVC, known as the centre of the neural basis of vestibular sensation. This might have been because visual inputs could be the only trigger of VIMS and because the visual system could be the sole centre of brain dynamics during the recovery phase.

Finally, the third possibility is that the increased functional connectivity in these brain regions during recovery from VIMS might reflect the maintenance of spatial memory. We

found increased connectivity between the cerebellar tonsil and parahippocampal gyrus (Supplementary Figure 1h). The parahippocampal gyrus has been suggested to be the centre of visual spatial information processing (Epstein *et al.*, 1998; Epstein, 2008) and is presumably related to the recognition and memorisation of the space where one exists. Previous resting-state fMRI studies of memory maintenance reported a significant increase in functional connectivity between the brain regions involved in memory processing after memory tasks (Tambini *et al.*, 2010; Gordon *et al.*, 2014). For example, in Tambini *et al.* (2010), the resting-state connectivity between the hippocampus and lateral occipital complex increased after associative memory tasks, which enabled the prediction of subsequent memory performance. Therefore, the increased connectivity in these regions might reflect novel spatial experiences in memory processing in the present participants with VIMS.

If change in functional connectivity is related to the neuroplastic changes and/or memory processing described above, then our findings might provide some insight into the neural process underlying the sensory conflict hypothesis (Reason & Brand, 1975; Reason, 1978; Oman, 1990). This hypothesis suggests that a conflict or mismatch among multiple sensory inputs, including visual and vestibular inputs, would cause MS. Interestingly, this hypothesis also indicates that a conflict not only among sensory inputs, but also between a sensory input and an empirically acquired sensory memory (so-called 'neural store') would cause MS. From this perspective, individuals with MS such as VIMS can develop adaptation, and tolerance increases when similar stimuli are repeated because of the reduced conflict between a sensory input and the 'neural store', which is the memory or plasticity acquired from the repeated sensory experience (Reason & Brand, 1975; Reason, 1978; Oman, 1990). Although the 'neural store' has been just a concept, the actual brain network associated with this concept may have been revealed by our findings. If so, these findings can advance our understanding of the neural mechanisms underlying the development of MS and adaptation to it.

Competing Interests

The authors declare that they have no conflict of interest related to this publication.

Author Contributions

J.M.: Conceptualisation, Formal analysis, Investigation, Writing - Original Draft, Writing - Review & Editing.

H.Y.: Project Administration, Supervision, Conceptualisation, Methodology, Writing - Original Draft, Writing - Review & Editing, Funding acquisition.

Y.I.: Supervision, Writing - Review.

H.Y., T.Y.: Methodology, Software support, Writing - Review.

T.M., M.U., T.H.: Methodology, Imaging, Writing - Review.

Data Accessibility

Data in this study are available upon request. Please contact the corresponding author for access.

Abbreviations

VIMS, visually induced motion sickness; MS, motion sickness; MRI, magnetic resonance imaging; fMRI, functional magnetic resonance imaging; SSQ, Simulator Sickness Questionnaire, ROI, region of interest; MT+, middle temporal complex.

References

Albert NB, Robertson EM, Mehta P, Miall RC (2009a) Resting state networks and memory consolidation. Communicative & integrative biology 2:530-532

Albert NB, Robertson EM, Miall RC (2009b) The Resting Human Brain and Motor Learning. Current Biology 19:1023-1027 doi: https://doi.org/10.1016/j.cub.2009.04.028

Bates D, Maechler M, Bolker B, Walker S (2015) lme4: Linear mixed-effects models using Eigen and S4. Journal of Statistical Software 67:1-48

Brandt T, Bartenstein P, Janek A, Dieterich M (1998) Reciprocal inhibitory visual-vestibular interaction. Visual motion stimulation deactivates the parieto-insular vestibular cortex. Brain 121:1749-1758 doi: 10.1093/brain/121.9.1749 %J Brain

Corbetta M, Akbudak E, Conturo TE, et al. (1998) A common network of functional areas for attention and eye movements. Neuron 21:761-773

Cox RW (1996) AFNI: software for analysis and visualization of functional magnetic resonance neuroimages. Computers and Biomedical research 29:162-173

Craig AD (2002) How do you feel? Interoception: the sense of the physiological condition of the body. Nature reviews neuroscience 3:655

Craig AD, Craig AD (2009) How do you feel--now? The anterior insula and human awareness. Nature reviews neuroscience 10

Crick FC, Koch C (2005) What is the function of the claustrum? Philosophical Transactions of the Royal Society of London B: Biological Sciences 360:1271-1279

Dieterich M, Bense S, Stephan T, Yousry TA, Brandt T (2003) fMRI signal increases and decreases in cortical areas during small-field optokinetic stimulation and central fixation. Experimental Brain Research 148:117-127

Dieterich M, Bucher SF, Seelos KC, Brandt T (1998) Horizontal or vertical optokinetic stimulation activates visual motion-sensitive, ocular motor and vestibular cortex areas with right hemispheric dominance. An fMRI study. Brain: a journal of neurology 121:1479-1495

Ebenholtz SM (1992) Motion sickness and oculomotor systems in virtual environments. Presence: Teleoperators & Virtual Environments 1:302-305

Ebenholtz SM, Cohen MM, Linder BJ (1994) The possible role of nystagmus in motion sickness: a hypothesis. Aviation, space, and environmental medicine 65:1032-1035

Epstein R, Kanwisher N (1998) A cortical representation of the local visual environment. Nature 392:598

Epstein RA (2008) Parahippocampal and retrosplenial contributions to human spatial navigation. Trends in cognitive sciences 12:388-396

Farmer AD, Ban VF, Coen SJ, et al. (2015) Visually induced nausea causes characteristic changes in cerebral, autonomic and endocrine function in humans. The Journal of physiology 593:1183-1196

Frank SM, Baumann O, Mattingley JB, Greenlee MW (2014) Vestibular and visual responses in human posterior insular cortex. Journal of neurophysiology 112:2481-2491

Frank SM, Wirth AM, Greenlee MW (2016) Visual-vestibular processing in the human Sylvian fissure. Journal of neurophysiology 116:263-271

Friston KJ, Frith CD, Liddle PF, Frackowiak RSJ (1993) Functional connectivity: the principal-component analysis of large (PET) data sets. Journal of Cerebral Blood

Flow & Metabolism 13:5-14
Gordon EM, Breeden AL, Bean SE, Vaidya CJ (2014) Working memory- related changes in functional connectivity persist beyond task disengagement. Human brain mapping 35:1004-1017
Gotts SJ, Simmons WK, Milbury LA, Wallace GL, Cox RW, Martin A (2012) Fractionation of social brain circuits in autism spectrum disorders. Brain 135:2711-2725
Hahsler M, Hornik K, Buchta C (2008) Getting things in order: an introduction to the R package seriation. Journal of Statistical Software 25:1-34
Kennedy RS, Drexler J, Kennedy RC (2010) Research in visually induced motion sickness. Applied ergonomics 41:494-503
Kennedy RS, Fowlkes JE, Lilienthal MG (1993a) Postural and performance changes following exposures to flight simulators. Aviation, Space, and Environmental Medicine
Kennedy RS, Lane NE, Berbaum KS, Lilienthal MG (1993b) Simulator sickness questionnaire: An enhanced method for quantifying simulator sickness. The international journal of aviation psychology 3:203-220
Kleinschmidt A, Thilo KV, Büchel C, Gresty MA, Bronstein AM, Frackowiak RSJ (2002) Neural correlates of visual-motion perception as object-or self-motion. Neuroimage 16:873-882
Klosterhalfen S, Pan F, Kellermann S, Enck P (2006) Gender and race as determinants of nausea induced by circular vection. Gender medicine 3:236-242
Konen CS, Kleiser R, Seitz RJ, Bremmer F (2005) An fMRI study of optokinetic nystagmus and smooth-pursuit eye movements in humans. Experimental Brain Research 165:203-216
Koslucher F, Haaland E, Malsch A, Webeler J, Stoffregen TA (2015) Sex differences in the incidence of motion sickness induced by linear visual oscillation. Aerospace medicine and human performance 86:787-793
Kuznetsova A, Brockhof BP, Christensen HBR (2017) lmerTest: Tests in Linear Mixed Effects Models. Journal of Statistical Software 82:1-26
Lewis CM, Baldassarre A, Committeri G, Romani GL, Corbetta M (2009) Learning sculpts the spontaneous activity of the resting human brain. Proceedings of the National Academy of Sciences:pnas-0902455106
Miyazaki J, Yamamoto H, Ichimura Y, et al. (2015) Inter-hemispheric desynchronization of the human MT+ during visually induced motion sickness. Experimental brain research 233:2421-2431
Munafo J, Diedrick M, Stoffregen TA (2017) The virtual reality head-mounted display Oculus Rift induces motion sickness and is sexist in its effects. Experimental brain research 235:889-901
Napadow V, Sheehan JD, Kim J, et al. (2012) The brain circuitry underlying the temporal evolution of nausea in humans. Cerebral cortex 23:806-813
Oman CM (1990) Motion sickness: a synthesis and evaluation of the sensory conflict theory. Canadian journal of physiology and pharmacology 68:294-303
Peltier SJ, LaConte SM, Niyazov DM, Liu JZ, Sahgal V, Yue GH, Hu XP (2005) Reductions in interhemispheric motor cortex functional connectivity after muscle fatigue. Brain research 1057:10-16
Reason JT (1978) Motion sickness adaptation: a neural mismatch model. Journal of the Royal Society of Medicine 71:819-829

Reason JT, Brand JJ (1975) Motion sickness. Academic press

Riccio GE, Stoffregen TA (1991) An ecological theory of motion sickness and postural instability. Ecological psychology 3:195-240

Shupak A, Gordon CR (2006) Motion sickness: advances in pathogenesis, prediction, prevention, and treatment. Aviation, space, and environmental medicine 77:1213-1223

Smith AT, Wall MB, Thilo KV (2011) Vestibular inputs to human motion-sensitive visual cortex. Cerebral cortex 22:1068-1077

Stanney K, Salvendy G (1998) Aftereffects and sense of presence in virtual environments: Formulation of a research and development agenda. International Journal of Human-Computer Interaction 10:135-187

Stevens WD, Buckner RL, Schacter DL (2009) Correlated low-frequency BOLD fluctuations in the resting human brain are modulated by recent experience in category-preferential visual regions. Cerebral cortex 20:1997-2006

Stevens WD, Tessler MH, Peng CS, Martin A (2015) Functional connectivity constrains the category- related organization of human ventral occipitotemporal cortex. Human brain mapping 36:2187-2206

Stoffregen TA, Chang C-H, Chen F-C, Zeng W-J (2017) Effects of decades of physical driving on body movement and motion sickness during virtual driving. PLoS one 12:e0187120

Suzuki R, Shimodaira H (2019) pvclust: Hierarchical Clustering with P-Values via Multiscale Bootstrap Resampling. Bioinformatics 22:1540-1542 doi: 10.1093/bioinformatics/btl117

Tambini A, Ketz N, Davachi L (2010) Enhanced brain correlations during rest are related to memory for recent experiences. Neuron 65:280-290

Team RC (2016) R: A language and environment for statistical computing. Vienna: R Foundation for Statistical Computing; 2014. In:

Toschi N, Kim J, Sclocco R, Duggento A, Barbieri R, Kuo B, Napadow V (2017) Motion sickness increases functional connectivity between visual motion and nausea-associated brain regions. Autonomic Neuroscience 202:108-113

Ujike H, Ukai K, Nihei K (2008) Survey on motion sickness-like symptoms provoked by viewing a video movie during junior high school class. Displays 29:81-89

Van Marle HJF, Hermans EJ, Qin S, Fernández G (2010) Enhanced resting-state connectivity of amygdala in the immediate aftermath of acute psychological stress. Neuroimage 53:348-354

Vohn R, Fimm B, Weber J, et al. (2007) Management of attentional resources in within-modal and cross- modal divided attention tasks: An fMRI study. Human brain mapping 28:1267-1275

Wall MB, Smith AT (2008) The representation of egomotion in the human brain. Current biology 18:191-194

Walter HJ, Li R, Munafo J, Curry C, Peterson N, Stoffregen TA (2019) Unstable coupling of body sway with imposed motion precedes visually induced motion sickness. Human Movement Science 64:389-397

Table Captions

Table 1. Statistical analysis of the degree of recovery in the subjective score of the Simulator Sickness Questionnaire (SSQ) (decrease in the SSQ between the post- and pre-rest phases)

This analysis was performed using a linear mixed-effects model with a within-participants fixed effect PHASE (Rest-1 *vs.* Rest-2 *vs.* Rest-3), a between-participants fixed effect GROUP (VIMS *vs.* the healthy participant group), an interaction of PHASE × GROUP, and a random effect of each individual participant. If there was a PHASE × GROUP interaction, *post hoc* analysis was conducted on the simple effect of PHASE. For the effect size of the interaction and the simple effect, *f*-squared and Cohen's *d* were computed, respectively. If there was no interaction, the main effect of PHASE was tested. The *P* values of the interaction were Bonferroni corrected for the number of scales of the SSQ, whereas those of the *post hoc* analyses were corrected for the number of the SSQ scales, participant groups, and comparison repetitions.

Table 2. Brain regions whose connectedness increased significantly during the recovery phase from visually induced motion sickness

Connectedness was computed using the AFNI software *3dTCorrMap* function separately for the 12 participants. These data were then transformed to the standard Talairach space. In this standard space, the connectedness was compared by use of the AFNI *3dLME* function, and the brain regions whose connectedness changed significantly during the recovery from VIMS were detected. Voxel-wise threshold $P < 0.0001$ and cluster level threshold $\alpha < 0.10$ were used.

Table 3. Brain region pairs whose functional connectivity increased during the recovery phase of visually induced motion sickness (VIMS) and the GROUP × PHASE interaction effect

A seed-based functional connectivity analysis revealed 19 brain region pairs whose

connectivities increased during the recovery from VIMS. The increases in connectivity were statistically tested with a linear mixed-effects model. The linear mixed-effects model had a within-participants fixed effect PHASE (Rest-1 *vs.* Rest-2 *vs.* Rest-3), a between-participants fixed effect GROUP (VIMS *vs.* the healthy participant group), interaction of PHASE × GROUP, and a random effect of each individual participant. For the effect size of the PHASE × GROUP interaction, *f*-squared was computed. The *P* values of the interaction were Bonferroni corrected for the number of brain region pairs. The numbering of the 19 pairs corresponds to that in Figure 4 and Supplementary Figure 1.

Table 4. Statistical analysis of the functional connectivity of brain region pairs for the visually induced motion sickness (VIMS) group

The linear mixed-effects model had a within-participants fixed effect PHASE (Rest-1 *vs.* Rest-2 *vs.* Rest-3), a between-participants fixed effect GROUP (VIMS *vs.* the healthy participant group), the interaction of PHASE × GROUP, and a random effect of each individual participant. Because there was a PHASE × GROUP interaction for all 19 brain pairs (Table 3), a *post hoc* test was conducted on the simple effect of PHASE. For the effect size of the simple effect, Cohen's *d* was computed. The *P* values of the *post hoc* tests were Bonferroni corrected for the number of brain region pairs, participant groups, and comparison repetitions. The numbering of the 19 pairs corresponds to that in Figure 4 and Supplementary Figure 1.

Table 5. Statistical analysis of the functional connectivity of brain region pairs for the healthy group

The description is the same as that of Table 4 but for the healthy participant group.

Supplementary Table 1. Statistical analysis of the effect of head movement on functional connectivity

The effect of head motion (maximum framewise displacement [FD]) on functional connectivity was statistically assessed by using a linear mixed-effects model, in which a within-participants fixed effect of FD and interactions of FD × PHASE and FD ×

GROUP were included, in addition to the fixed effects of PHASE, GROUP, and PHASE × GROUP and a random effect of each individual participant. If the head movement-related interactions (i.e., FD × PHASE and FD × GROUP) were statistically significant, the statistics for FD were omitted because it was difficult to determine the effect.

Figure Captions

Figure 1. Schematic diagram showing the time course of the experimental session

After the first rest phase (Rest-1), the local motion stimulus was presented as a control. After the second rest phase (Rest-2), the global motion stimulus, which can induce visually induced motion sickness (VIMS), was presented. Finally, the third rest phase (Rest-3) comprised the recovery from VIMS.

Figure 2. Time course of the change in the Total Score (TS) of the Simulator Sickness Questionnaire (SSQ)

The vertical axis shows the change in the TS (post-score minus pre-score) of the SSQ. The horizontal axis shows the experimental phase (Rest-1, Rest-2, and Rest-3). The visually induced motion sickness (VIMS) group's participants experienced motion sickness soon before the third rest phase (Rest-3), and recovery from symptoms occurred during Rest-3. Accordingly, the score of the VIMS group (solid line) significantly decreased before and after Rest-3, whereas the score of the healthy group participants (broken line), who did not experience VIMS, did not change as much.

Figure 3. Twelve brain regions whose connectedness significantly increased during the recovery phase from visually induced motion sickness (VIMS)

Each row is as follows: a, left thalamus; b, anterior cingulate; c, left insula; d, right insula; e, cerebellar tonsil; f, claustrum; g, right lingual gyrus; h, cingulate gyrus; i, right thalamus; j, left superior frontal gyrus; k, left lingual gyrus; and l, inferior frontal gyrus. Each column shows, from left to right, axial, sagittal, and coronal brain images. The following thresholds were set: voxel-wise threshold $P < 0.0001$, cluster level threshold $\alpha < 0.10$.

Figure 4. Brain regions whose functional connectivity with the seed regions increased in the recovery phase from visually induced motion sickness (VIMS)

Each column shows, from left to right, axial, sagittal, and coronal brain images, and the change in the functional connectivity (Z scores averaged within the participants' groups) of each experimental phase, separately for VIMS and healthy groups, respectively (error bars are standard errors). Each panel is the result for the following brain regions (the brain region in brackets is the corresponding seed): a–left superior temporal gyrus (right insula), b–right inferior parietal lobule (right claustrum), c–left superior temporal gyrus (right claustrum), d–left inferior parietal lobule (right claustrum); and e–left lentiform nucleus (left superior frontal gyrus). For this mapping, we used the following thresholds: voxel-wise threshold $P < 0.0001$, cluster level threshold $\alpha < 0.05$. The numbering of brain region pairs corresponds to that in Tables 3, 4, and 5.

Figure 5. Correlation plots between the change in the Total Score (TS) of the Simulator Sickness Questionnaire (SSQ) and the change in functional connectivity

The vertical axis is the change in the TS of the SSQ: Rest-3 minus the average of Rest-1 and Rest-2; the greater the recovery in VIMS symptoms, the greater the decrease in this score. The horizontal axis is the change in functional connectivity: Rest-3 minus the average of Rest-1 and Rest-2. In the graphs, ρ indicates Spearman's rank correlation coefficient, with the corresponding *P* value shown below. The *P* values were Bonferroni corrected for multiple comparisons among the 19 brain region pairs. Abbreviations: IPL, inferior parietal lobule; L, left; R, right; SFG, superior frontal gyrus; STG, superior temporal gyrus.

Figure 6. Hierarchical clustering trees of the 12 brain regions showing recovery-selective increases in connectedness

(a) The dendrogram of the VIMS group for the recovery phase (Rest-3), which was derived from the distance matrix (Supplementary Fig. 2a), whose elements indicate 1 minus absolute partial correlation between each pair of the 12 regions. Statistically significant clusters are marked with an asterisk ($P < 0.05$) or plus ($P < 0.1$). Brain regions showing recovery-selective increases in the ROI-based functional connectivity and

correlations with SSQ are underlined and in italics, respectively. (b) The same as (a) but for the healthy group. (c) The same as (a) but for the control phase (the average of Rest-1 and Rest-2). (d) The same as (c) but for the healthy group. Abbreviations: L, left; R, right; LG, lingual gyrus; SFG, superior frontal gyrus; IFG, inferior frontal gyrus.

Supplementary Figure 1. Brain regions whose functional connectivity with the seed regions increased in the recovery phase from visually induced motion sickness (VIMS)

Each column shows, from left to right, axial, sagittal, and coronal brain images, and the change in functional connectivity (Z scores averaged within the participants' groups) of each experimental phase, separately for VIMS and healthy groups, respectively (error bars are standard errors). Each panel is the result for the following brain regions (the brain region in brackets is the corresponding seed): a–right insula (right thalamus), b–right inferior parietal lobule (right thalamus), c–right declive (right thalamus), d–left thalamus (left insula), e–right inferior parietal lobule (left insula), f–left thalamus (right insula), g–left inferior temporal gyrus (right insula), h–left parahippocampal gyrus (left cerebellar tonsil), i–left cingulate gyrus (right claustrum), j–left inferior frontal gyrus (right claustrum), k–right insula (left cingulate gyrus), l–left medial frontal gyrus (left superior frontal gyrus), m–left middle temporal gyrus (left superior frontal gyrus), and n–left inferior frontal gyrus (right inferior frontal gyrus). For this mapping, we used the following thresholds: voxel-wise threshold $P < 0.0001$, cluster level threshold $\alpha < 0.05$. The numbering of brain region pairs corresponds to that in Tables 3, 4, and 5.

Supplementary Figure 2. Distance matrices of the 12 brain regions showing recovery-selective increases in connectedness

(a) The distance matrix of the VIMS group for the recovery phase (Rest-3), whose elements indicate 1 minus absolute partial correlation between each pair of the 12 regions. Brain regions showing recovery-selective increases in the ROI-based functional connectivity and correlations with SSQ are underlined and in italics, respectively. (b) The same as (a) but for the healthy group. (c) The same as (a) but for the control phase (the

average of Rest-1 and Rest-2). (d) The same as (c) but for the healthy group. Abbreviations: L, left; R, right; LG, lingual gyrus; SFG, superior frontal gyrus; IFG, inferior frontal gyrus.

Supplementary Figure 3. Statistically independent brain networks related to recovery from visually induced motion sickness (VIMS)

(a) The within-participant averaged distance matrix for the recovery phase of the VIMS group. Each element represents a cross-correlation coefficient between each pair of the 22 regions determined by a dictionary learning technique. This analysis derived 22 regions of interest (ROIs). (b) The top 10% connections derived from the distance matrix. The connections are overlaid on a glass brain. Yellow circles and red lines denote the derived regions and connections, respectively. The connections are as follows: R Posterior Cingulate–L Lingual Gyrus, L Lingual Gyrus–R MOG, L Lingual Gyrus–L MTG, L Lingual Gyrus–R MOG, L Lingual Gyrus–L MOG, R Superior Occipital Gyrus–R MOG, R Culmen–R Parahippocampal Gyrus, R Culmen–R Cuneus, R Culmen–L Cuneus, R Culmen–R MOG, R Culmen–L MOG, R Parahippocampal Gyrus–L Cuneus, R Parahippocampal Gyrus–L Posterior Cingulate, R Cuneus–L Cuneus, R Cuneus–L Precuneus, L Cuneus–R MOG, R MOG–L MTG, L MOG–R MOG, L MOG–R MOG, L MTG–R MOG, L MTG–L MOG, and R MOG–R MOG. Abbreviations: L, left; R, right; MTG, middle temporal gyrus; MOG, middle occipital gyrus.

Table 1. Statistical analysis of the degree of recovery in the subjective score of the Simulator Sickness Questionnaire (SSQ) (decrease in the SSQ between the post- and pre-rest phases)

Scale	GROUP × PHASE interaction		Simple effect of PHASE						
				VIMS			Healthy		
	Statistics P value (χ^2)	Effect size f^2		Coefficient Estimate ± SE	Statistics P value (χ^2)	Effect size Cohen's d	Coefficient Estimate ± SE	Statistics P value (χ^2)	Effect size Cohen's d
Total score	.005 (13.30)	0.45	Rest-1 vs. Rest-2	46.75 ± 11.45	> 1 (0.03)	0.07	-4.99 ± 2.29	.417 (4.72)	0.89
			Rest-2 vs. Rest-3	-41.76 ± 10.77	.001 (15.04)	1.58	-0.62 ± 2.29	> 1 (0.07)	0.11
			Rest-1 vs. Rest-3	-43.63 ± 10.77	0.0007 (16.41)	1.65	-5.61 ± 2.29	.203 (5.98)	1.00
Disorientation	.0002 (19.16)	0.72	Rest-1 vs. Rest-2	-2.32 ± 15.09	> 1 (0.02)	0.06	-2.32 ± 3.19	> 1 (0.53)	0.30
			Rest-2 vs. Rest-3	-64.96 ± 15.09	0.0002 (18.52)	1.76	2.32 ± 3.19	> 1 (< 0.01)	0.30
			Rest-1 vs. Rest-3	-67.28 ± 15.09	0.0001 (19.87)	1.82	-5.92 ± 3.19	> 1 (0.52)	< 0.01

Scale			Main effect of PHASE		
			Coefficient Estimate ± SE	Statistics P value (χ2)	Effect size Cohen's d
Nausea	.084 (7.74)	0.24	-7.16 ± 3.46	.539 (4.28)	0.6
Oculomotor	.259 (5.48)	0.16	-4.21 ± 1.96	.444 (4.62)	0.62

This analysis was performed using a linear mixed-effects model with a within-participants fixed effect PHASE (Rest-1 vs. Rest-2 vs. Rest-3), a between-participants fixed effect GROUP (VIMS vs. the healthy participant group), an interaction of PHASE × GROUP, and a random effect of each individual participant. If there was a PHASE × GROUP interaction, post hoc analysis was conducted on the simple effect of PHASE. For the effect size of the interaction and the simple effect, f-squared and Cohen's d were computed, respectively. If there was no interaction, the main effect of PHASE was tested. The P values of the interaction were Bonferroni corrected for the number of scales of the SSQ, whereas those of the post hoc analyses were

Table 2. Brain regions whose connectedness increased significantly during the recovery phase from visually induced motion sickness

	Cluster label	Hemisphere	Voxel	Talairach coordinate			Broadman area	Cluster level α
				x	y	z		
1	Thalamus	Left	131	+4.5	+19.5	+8.5	–	≪0.01
2	Anterior Cingulate	Right	49	−22.5	−43.5	+8.5	9, 10	≪0.01
3	Insula	Left	41	+40.5	−10.5	+5.5	13, 44	≪0.01
4	Insula	Right	25	−31.5	−13.5	+8.5	13	<0.01
5	Cerebellar Tonsil	Left	21	+13.5	+43.5	−39.5	-	<0.01
6	Claustrum	Right	16	−25.5	+19.5	+17.5	13	<0.01
7	Lingual Gyrus	Right	11	−4.5	+91.5	−3.5	17, 18	<0.03
8	Cingulate Gyrus	Left	10	+1.5	−19.5	+35.5	6, 32	<0.03
9	Thalamus	Right	7	−22.5	+31.5	+8.5	30	<0.06
10	Superior Frontal Gyrus	Left	7	+25.5	−40.5	+14.5	9, 10, 32	<0.06
11	Lingual Gyrus	Left	6	+13.5	+94.5	−12.5	17, 18	<0.07
12	Inferior Frontal Gyrus	Right	6	−28.5	−10.5	+26.5	-	<0.07

Connectedness was computed using the AFNI software 3dTCorrMap function separately for the 12 participants. These data were then transformed to the standard Talairach space. In this standard space, the connectedness was compared by use of the AFNI 3dLME function, and the brain regions whose connectedness changed significantly during the recovery from VIMS were detected. Voxel-wise threshold $P < 0.0001$, cluster level threshold $\alpha < 0.10$ were used.

Table 3. Brain region pairs whose functional connectivity increased during the recovery phase of visually induced motion sickness (VIMS) and the GROUP × PHASE interaction effect

Seed label		Cluster label	Hemisphere	GROUP × PHASE interaction		Voxel	Talairach coordinate			Broadman area
				Test statistics P value (χ^2)	Effect size f^2		x	y	z	
L Thalamus	1	Insula	Right	.003 (17.45)	0.11	21	−34.5	−13.5	+2.5	13, 47
	2	Inferior Parietal Lobule	Right	.014 (14.48)	0.12	9	−55.5	+28.5	+26.5	2, 13, 40
	3	Declive	Right	.0003 (20.12)	0.10	8	−4.5	+58.5	−12.5	–
L Insula	4	Thalamus	Left	.001 (18.99)	0.11	15	+4.5	+10.5	+11.5	–
	5	Inferior Parietal Lobule	Right	.004 (16.93)	0.28	9	−58.5	+28.5	+29.5	2, 40
R Insula	6	Thalamus	Left	5×10^{-5} (25.78)	0.15	23	+7.5	+16.5	+5.5	–
	7	Superior Temporal Gyrus	Left	.002 (18.81)	0.16	13	+55.5	+31.5	+11.5	22, 41, 42
	8	Inferior Temporal Gyrus	Left	.001 (19.26)	0.21	9	+49.5	+58.5	−9.5	19, 20, 37
L Cerebellar Tonsil	9	Parahippocampal Gyrus	Left	.005 (16.37)	0.18	11	+16.5	+16.5	−15.5	–
R Claustrum	10	Cingulate Gyrus	Left	.0004 (21.52)	0.27	83	+1.5	−22.5	+26.5	24, 32
	11	Inferior Parietal Lobule	Right	.002 (18.72)	0.23	22	−55.5	+31.5	+26.5	13, 40, 42
	12	Inferior Frontal Gyrus	Left	.003 (17.45)	0.24	17	+40.5	−25.5	+2.5	13, 45, 47
	13	Superior Temporal Gyrus	Left	.0002 (23.07)	0.21	11	+58.5	+25.5	+11.5	22, 40, 41, 42
	14	Inferior Parietal Lobule	Left	.004 (16.95)	0.13	8	+55.5	+34.5	+23.5	13, 40, 42
L Cingulate Gyrus	15	Insula	Right	5×10^{-5} (25.62)	0.23	19	−25.5	+25.5	+20.5	13
L Superior Frontal Gyrus	16	Medial Frontal Gyrus	Left	5×10^{-5} (25.53)	0.20	67	+4.5	−25.5	+41.5	8, 32
	17	Middle Temporal Gyrus	Left	.004 (17.16)	0.30	12	+46.5	+52.5	−0.5	19, 37
	18	Lentiform Nucleus	Left	.0001 (17.72)	0.29	8	+28.5	+19.5	+11.5	13
R Inferior Frontal Gyrus	19	Inferior Frontal Gyrus	Left	.002 (18.80)	0.31	14	+40.5	−28.5	−0.5	13, 45, 47

A seed-based functional connectivity analysis revealed 19 brain region pairs whose connectivities increased during the recovery from VIMS. The increases in connectivity were statistically tested with a linear mixed-effects model. The linear mixed-effects model had a within-participants fixed effect PHASE (Rest-1 vs. Rest-2 vs. Rest-3), a between-participants fixed effect GROUP (VIMS vs. the healthy participant group), interaction of PHASE × GROUP, and a random effect of each individual participant. For the effect size of the PHASE × GROUP interaction, f-squared was computed. The P values of the interaction were Bonferroni corrected for the number of brain region pairs. The numbering of the 19 pairs corresponds to that in Figure 4 and Supplementary Figure 1.

Table 4. Statistical analysis of the functional connectivity of brain region pairs for the visually induced motion sickness (VIMS) group

				Rest-1 vs. Rest-2			Rest-2 vs. Rest-3			Rest-1 vs. Rest-3		
				Coefficient Estimate ± SE	**Test statistics** *P* value (χ^2)	**Effect size** Cohen's *d*	**Coefficient** Estimate ± SE	**Test statistics** *P* value (χ^2)	**Effect size** Cohen's *d*	**Coefficient** Estimate ± SE	**Test statistics** *P* value (χ^2)	**Effect size** Cohen's *d*
L Thalamus	1 Insula	Right	−0.07 ± 0.07	> 1 (1.05)	0.42	0.34 ± 0.07	5×10^{-5} (25.70)	2.07	0.27 ± 0.07	.006 (16.37)	1.65
	2 Inferior Parietal Lobule	Right	−0.04 ± 0.06	> 1 (0.44)	0.27	0.30 ± 0.06	4×10^{-5} (25.94)	2.08	0.26 ± 0.06	.001 (19.61)	1.81
	3 Declive	Right	−0.03 ± 0.04	> 1 (0.82)	0.37	0.27 ± 0.04	3×10^{-12} (57.83)	3.10	0.24 ± 0.04	2×10^{-9} (44.86)	2.73
L Insula	4 Thalamus	Left	0.02 ± 0.05	> 1 (0.10)	0.13	0.27 ± 0.05	2×10^{-6} (32.17)	2.32	0.29 ± 0.05	2×10^{-7} (35.93)	2.45
	5 Inferior Parietal Lobule	Right	−0.04 ± 0.07	> 1 (0.35)	0.24	0.43 ± 0.07	8×10^{-8} (38.05)	2.52	0.39 ± 0.07	3×10^{-6} (31.12)	2.28
R Insula	6 Thalamus	Left	−0.06 ± 0.05	> 1 (1.39)	0.48	0.40 ± 0.05	2×10^{-11} (53.99)	3.00	0.34 ± 0.05	8×10^{-8} (38.05)	2.52
	7 Superior Temporal Gyrus	Left	0.11 ± 0.08	> 1 (2.13)	0.60	0.30 ± 0.08	.010 (15.40)	1.60	0.41 ± 0.08	.0003 (29.00)	2.20
	8 Inferior Temporal Gyrus	Left	0.11 ± 0.07	> 1 (2.79)	0.68	0.26 ± 0.07	.016 (14.53)	1.56	0.38 ± 0.07	5×10^{-6} (30.05)	2.24
L Cerebellar Tonsil	9 Parahippocampal Gyrus	Left	−0.003 ± 0.08	> 1 (0.001)	0.01	0.32 ± 0.08	.008 (15.92)	1.63	0.32 ± 0.08	.009 (15.65)	1.62
R Claustrum	10 Cingulate Gyrus	Left	−0.01 ± 0.06	> 1 (0.05)	0.09	0.33 ± 0.06	3×10^{-6} (31.22)	2.28	0.32 ± 0.06	9×10^{-6} (28.86)	2.19
	11 Inferior Parietal Lobule	Right	−0.06 ± 0.07	> 1 (0.64)	0.33	0.33 ± 0.07	.0002 (22.58)	1.94	0.27 ± 0.07	.009 (15.60)	1.61
	12 Inferior Frontal Gyrus	Left	−0.004 ± 0.05	> 1 (0.01)	0.03	0.29 ± 0.05	5×10^{-6} (30.03)	2.24	0.28 ± 0.05	8×10^{-6} (29.17)	2.21
	13 Superior Temporal Gyrus	Left	0.11 ± 0.07	> 1 (2.30)	0.62	0.27 ± 0.07	.019 (14.19)	1.54	0.38 ± 0.07	1×10^{-5} (27.91)	2.16
	14 Inferior Parietal Lobule	Left	0.01 ± 0.06	> 1 (0.01)	0.04	0.26 ± 0.06	.002 (18.80)	1.77	0.27 ± 0.06	.001 (19.67)	1.81
L Cingulate Gyrus	15 Insula	Right	−0.002 ± 0.07	> 1 (0.002)	0.02	0.35 ± 0.07	1×10^{-5} (28.37)	2.17	0.34 ± 0.07	1×10^{-5} (27.97)	2.16
L Superior Frontal Gyrus	16 Medial Frontal Gyrus	Left	0.04 ± 0.06	> 1 (0.51)	0.29	0.26 ± 0.06	.0003 (22.06)	1.92	0.31 ± 0.06	7×10^{-6} (29.29)	2.21
	17 Middle Temporal Gyrus	Left	0.06 ± 0.07	> 1 (0.68)	0.34	0.25 ± 0.07	.090 (11.26)	1.37	0.31 ± 0.07	.003 (17.45)	1.71
	18 Lentiform Nucleus	Left	0.10 ± 0.07	> 1 (1.71)	0.53	0.27 ± 0.07	.026 (13.60)	1.51	0.37 ± 0.07	7×10^{-5} (24.96)	2.04
R Inferior Frontal Gyrus	19 Inferior Frontal Gyrus	Left	0.001 ± 0.05	> 1 (0.0004)	0.01	0.24 ± 0.05	2×10^{-5} (27.66)	2.15	0.24 ± 0.05	1×10^{-5} (27.87)	2.16

The linear mixed-effects model had a within-participants fixed effect PHASE (Rest-1 vs. Rest-2 vs. Rest-3), a between-participants fixed effect GROUP (VIMS vs. the healthy participant group), the interaction of PHASE × GROUP, and a random effect of each individual participant. Because there was a PHASE × GROUP interaction for all 19 brain pairs (Table 3), a post hoc test was conducted on the simple effect of PHASE. For the effect size of the simple effect, Cohen's d was computed. The P values of the post hoc tests were Bonferroni corrected for the number of brain region pairs, participant groups, and comparison repetitions. The numbering of the 19 pairs corresponds to that in Figure 4 and Supplementary Figure 1.

Table 5. Statistical analysis of the functional connectivity of brain region pairs for the healthy group

				Rest-1 vs. Rest-2			Rest-2 vs. Rest-3			Rest-1 vs. Rest-3		
				Coefficient Estimate ± SE	**Test statistics** *P* value (χ^2)	**Effect size** Cohen's *d*	**Coefficient** Estimate ± SE	**Test statistics** *P* value (χ^2)	**Effect size** Cohen's *d*	**Coefficient** Estimate ± SE	**Test statistics** *P* value (χ^2)	**Effect size** Cohen's *d*
L Thalamus	1	Insula	Right	−0.01 ± 0.05	> 1 (0.07)	0.11	−0.06 ± 0.05	> 1 (1.25)	0.46	−0.07 ± 0.05	> 1 (1.92)	0.57
	2	Inferior Parietal Lobule	Right	−0.06 ± 0.07	> 1 (0.66)	0.33	−0.05 ± 0.07	> 1 (0.49)	0.29	−0.11 ± 0.07	> 1 (2.30)	0.62
	3	Declive	Right	−0.04 ± 0.06	> 1 (0.59)	0.31	−0.05 ± 0.06	> 1 (0.82)	0.37	−0.10 ± 0.06	> 1 (2.79)	0.68
L Insula	4	Thalamus	Left	−0.07 ± 0.07	> 1 (1.13)	0.43	−0.06 ± 0.07	> 1 (0.90)	0.39	−0.14 ± 0.07	> 1 (4.05)	0.82
	5	Inferior Parietal Lobule	Right	−0.11 ± 0.07	> 1 (2.30)	0.62	−0.04 ± 0.07	> 1 (0.24)	0.20	−0.07 ± 0.07	> 1 (1.05)	0.42
R Insula	6	Thalamus	Left	−0.02 ± 0.05	> 1 (0.13)	0.15	−0.04 ± 0.05	> 1 (0.88)	0.38	−0.06 ± 0.05	> 1 (1.70)	0.53
	7	Superior Temporal Gyrus	Left	0.02 ± 0.06	> 1 (0.08)	0.11	−0.09 ± 0.06	> 1 (2.25)	0.61	−0.07 ± 0.06	> 1 (1.50)	0.50
	8	Inferior Temporal Gyrus	Left	−0.05 ± 0.05	> 1 (1.03)	0.41	−0.04 ± 0.05	> 1 (0.45)	0.27	−0.09 ± 0.05	> 1 (2.84)	0.69
L Cerebellar Tonsil	9	Parahippocampal Gyrus	Left	−0.05 ± 0.07	> 1 (0.45)	0.27	−0.10 ± 0.07	> 1 (2.12)	0.59	−0.15 ± 0.07	> 1 (4.51)	0.87
R Claustrum	10	Cingulate Gyrus	Left	−0.03 ± 0.05	> 1 (0.41)	0.26	−0.06 ± 0.05	> 1 (1.29)	0.46	−0.09 ± 0.05	> 1 (3.15)	0.72
	11	Inferior Parietal Lobule	Right	0.01 ± 0.06	> 1 (0.06)	0.10	−0.12 ± 0.06	> 1 (4.20)	0.84	−0.11 ± 0.06	> 1 (3.26)	0.74
	12	Inferior Frontal Gyrus	Left	−0.08 ± 0.06	> 1 (1.63)	0.52	−0.03 ± 0.06	> 1 (0.25)	0.20	−0.11 ± 0.06	> 1 (3.14)	0.72
	13	Superior Temporal Gyrus	Left	−0.08 ± 0.04	> 1 (4.84)	0.90	−0.04 ± 0.04	> 1 (1.06)	0.42	−0.11 ± 0.04	.142 (10.43)	1.32
	14	Inferior Parietal Lobule	Left	−0.07 ± 0.05	> 1 (2.00)	0.58	−0.04 ± 0.05	> 1 (0.46)	0.27	−0.11 ± 0.05	> 1 (4.34)	0.85
L Cingulate Gyrus	15	Insula	Right	−0.06 ± 0.04	> 1 (2.55)	0.65	−0.06 ± 0.04	> 1 (2.69)	0.67	−0.12 ± 0.04	.137 (10.49)	1.32
L Superior Frontal Gyrus	16	Medial Frontal Gyrus	Left	0.003 ± 0.03	> 1 (0.02)	0.06	−0.08 ± 0.03	.313 (8.97)	1.22	−0.08 ± 0.03	.502 (8.11)	1.16
	17	Middle Temporal Gyrus	Left	−0.06 ± 0.05	> 1 (1.33)	0.47	−0.06 ± 0.05	> 1 (0.70)	0.53	−0.12 ± 0.05	> 1 (6.04)	1.00
	18	Lentiform Nucleus	Left	−0.04 ± 0.06	> 1 (0.50)	0.29	−0.07 ± 0.06	> 1 (1.15)	0.44	−0.11 ± 0.06	> 1 (3.18)	0.73
R Inferior Frontal Gyrus	19	Inferior Frontal Gyrus	Left	−0.02 ± 0.05	> 1 (0.14)	0.15	−0.07 ± 0.05	> 1 (1.70)	0.53	−0.09 ± 0.05	> 1 (2.81)	0.68

The description is the same as that of Table 4 but for the healthy participant group.

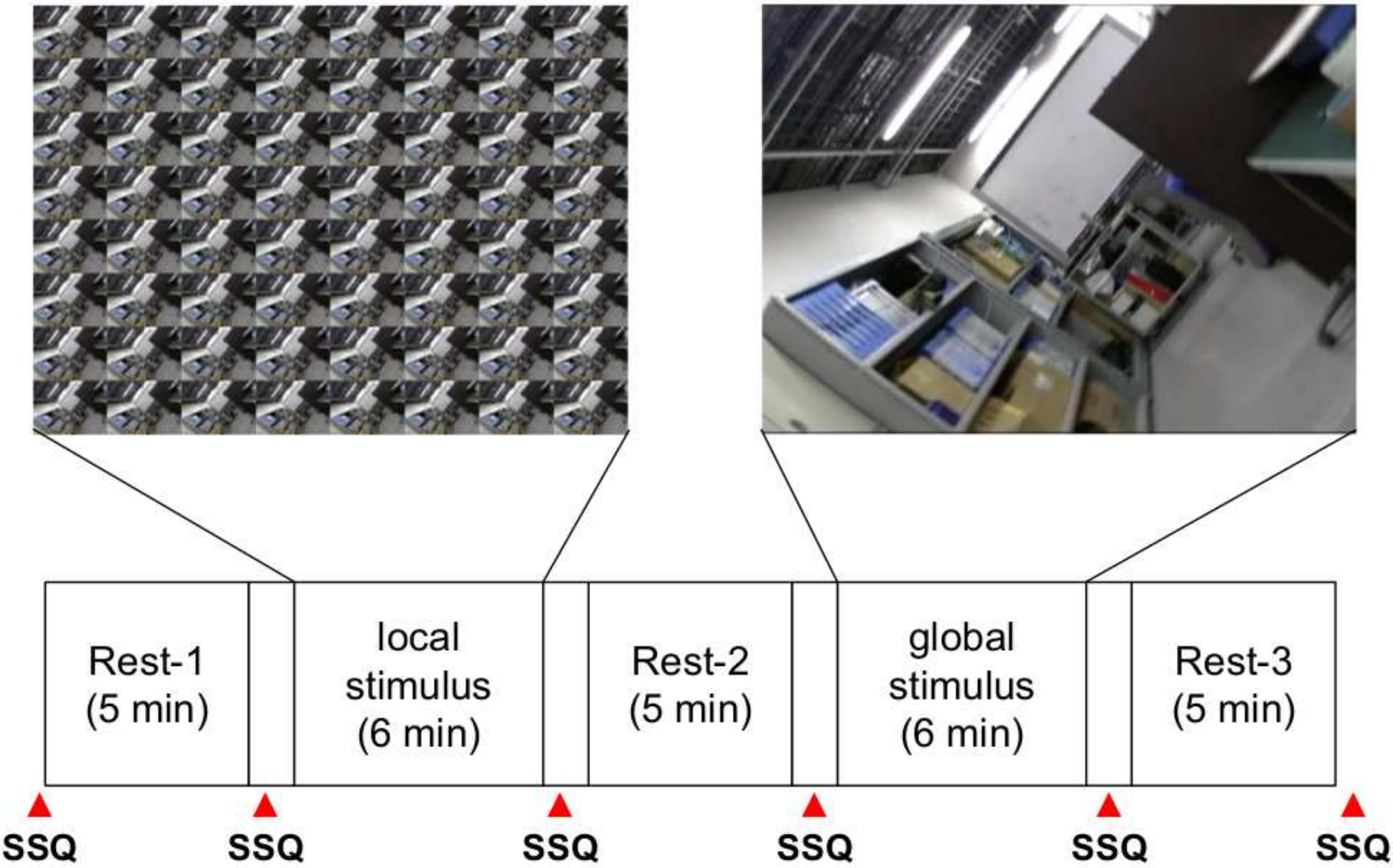

Figure 1. Schematic diagram showing the time course of the experimental session
After the first rest phase (Rest-1), the local motion stimulus was presented as a control. After the second rest phase (Rest-2), the global motion stimulus, which can induce visually induced motion sickness (VIMS), was presented. Finally, the third rest phase (Rest-3) comprised the recovery from VIMS.

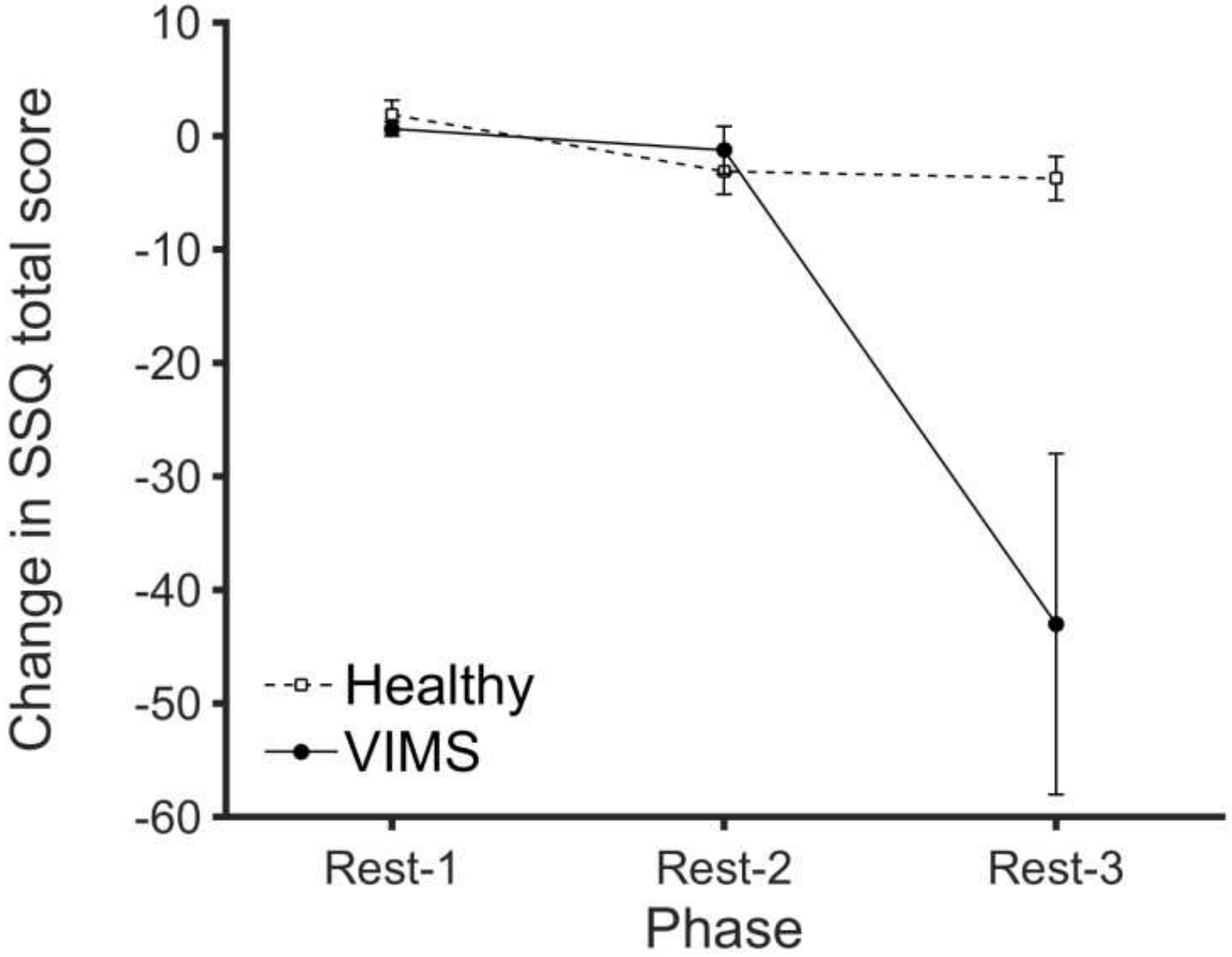

Figure 2. Time course of the change in the Total Score (TS) of the Simulator Sickness Questionnaire (SSQ)
The vertical axis shows the change in the TS (post-score minus pre-score) of the SSQ. The horizontal axis shows the experimental phase (Rest-1, Rest-2, and Rest-3). The visually induced motion sickness (VIMS) group's participants experienced motion sickness soon before the third rest phase (Rest-3), and recovery from symptoms occurred during Rest-3. Accordingly, the score of the VIMS group (solid line) significantly decreased before and after Rest-3, whereas the score of the healthy group participants (broken line), who did not experience VIMS, did not change as much.

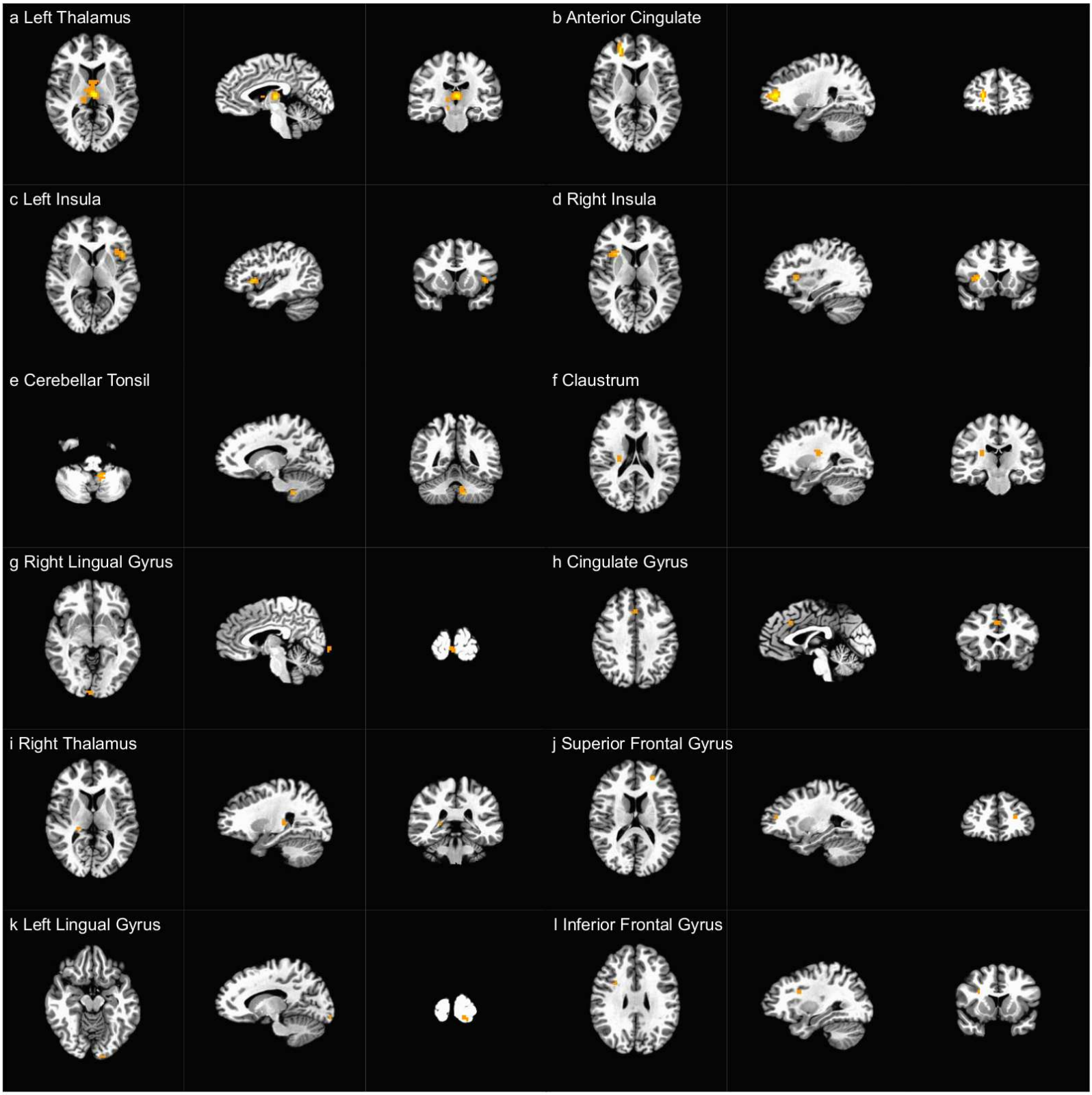

Figure 3. Twelve brain regions whose connectedness significantly increased during the recovery phase from visually induced motion sickness (VIMS)

Each row is as follows: a, left thalamus; b, anterior cingulate; c, left insula; d, right insula; e, cerebellar tonsil; f, claustrum; g, right lingual gyrus; h, cingulate gyrus; i, right thalamus; j, left superior frontal gyrus; k, left lingual gyrus; and l, inferior frontal gyrus. Each column shows, from left to right, axial, sagittal, and coronal brain images. The following thresholds were set: voxel-wise threshold $P < 0.0001$, cluster level threshold $\alpha < 0.10$.

a

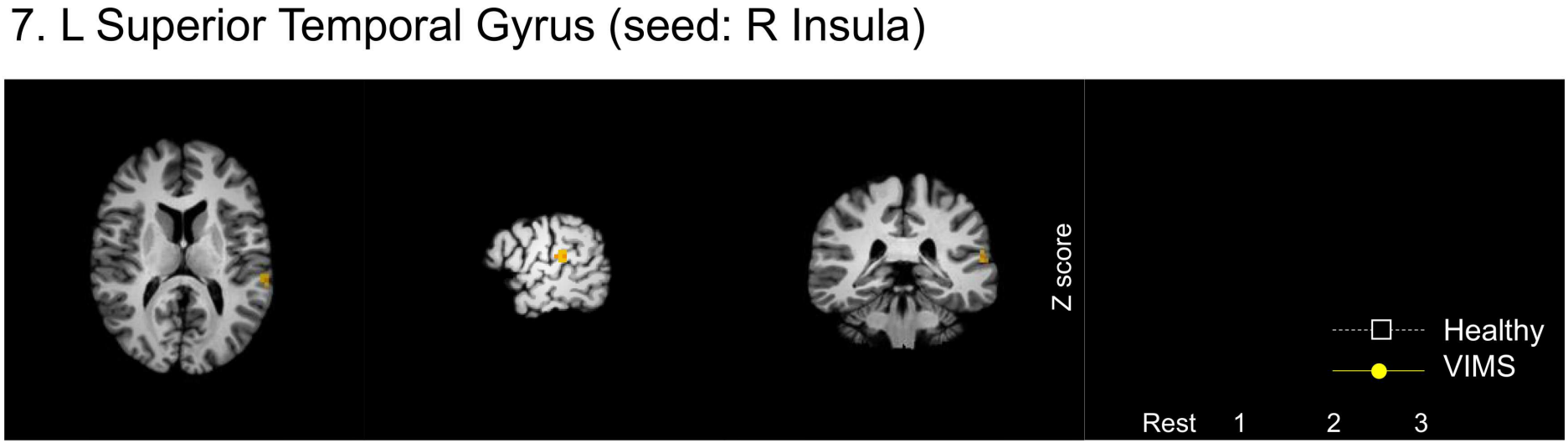

Figure 4. Brain regions whose functional connectivity with the seed regions increased in the recovery phase from visually induced motion sickness (VIMS)

Each column shows, from left to right, axial, sagittal, and coronal brain images, and the change in the functional connectivity (Z scores averaged within the participants' groups) of each experimental phase, separately for VIMS and healthy groups, respectively (error bars are standard errors). Each panel is the result for the following brain regions (the brain region in brackets is the corresponding seed): a–left superior temporal gyrus (right insula), b–right inferior parietal lobule (right claustrum), c–left superior temporal gyrus (right claustrum), d–left inferior parietal lobule (right claustrum); and e–left lentiform nucleus (left superior frontal gyrus). For this mapping, we used the following thresholds: voxel-wise threshold $P < 0.0001$, cluster level threshold $\alpha < 0.05$. The numbering of brain region pairs corresponds to that in Tables 3, 4, and 5.

b 11. R Inferior Parietal Lobule (seed: R Claustrum)

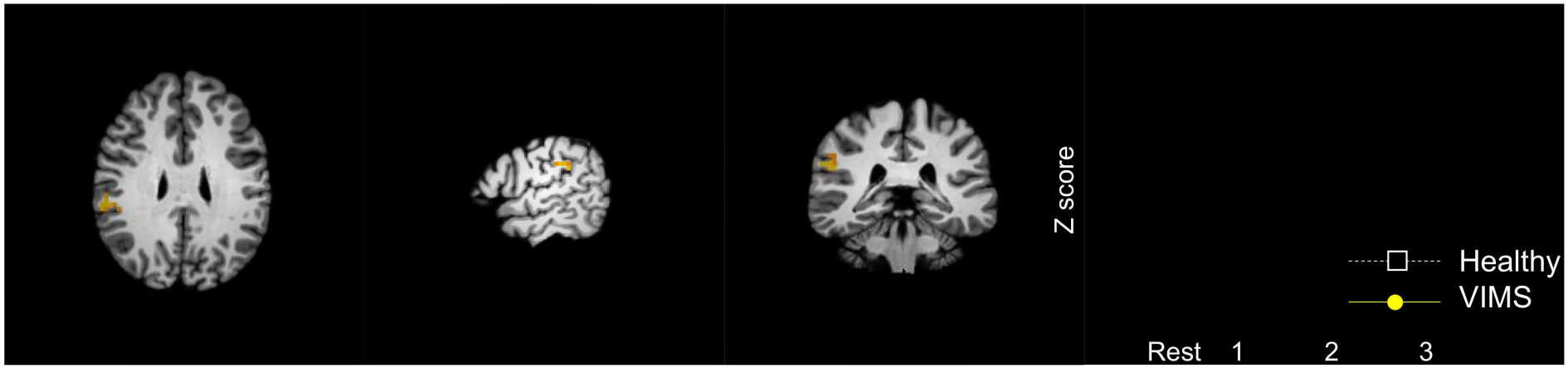

Figure 4. Brain regions whose functional connectivity with the seed regions increased in the recovery phase from visually induced motion sickness (VIMS)

The same as Figure 4a but for right inferior parietal lobule.

c 13. L Superior Temporal Gyrus (seed: R Claustrum)

Figure 4. Brain regions whose functional connectivity with the seed regions increased in the recovery phase from visually induced motion sickness (VIMS)

The same as Figure 4a but for left superior temporal gyrus.

d 14. L Inferior Parietal Lobule (seed: R Claustrum)

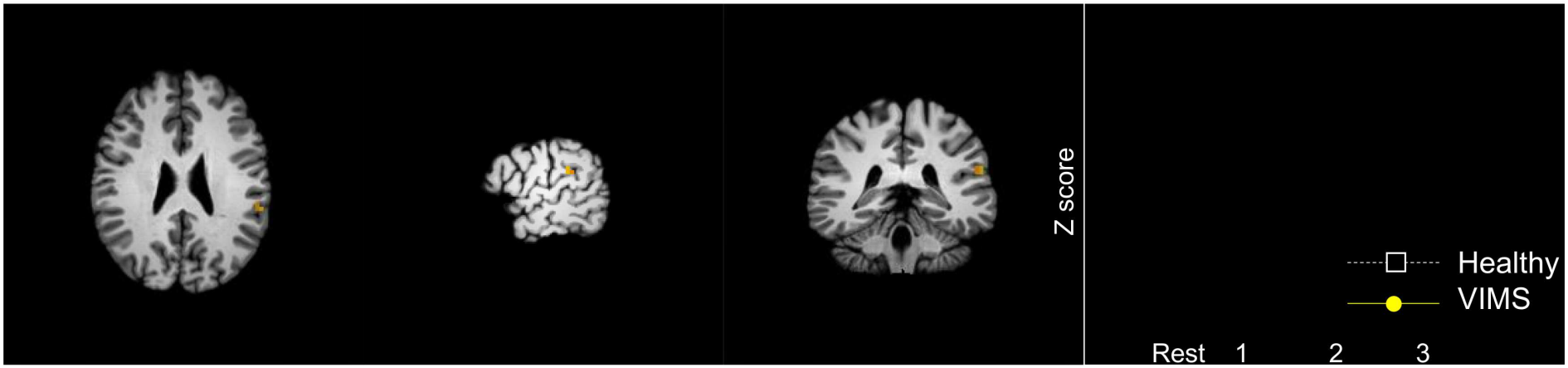

Figure 4. Brain regions whose functional connectivity with the seed regions increased in the recovery phase from visually induced motion sickness (VIMS)

The same as Figure 4a but for left inferior parietal lobule.

e

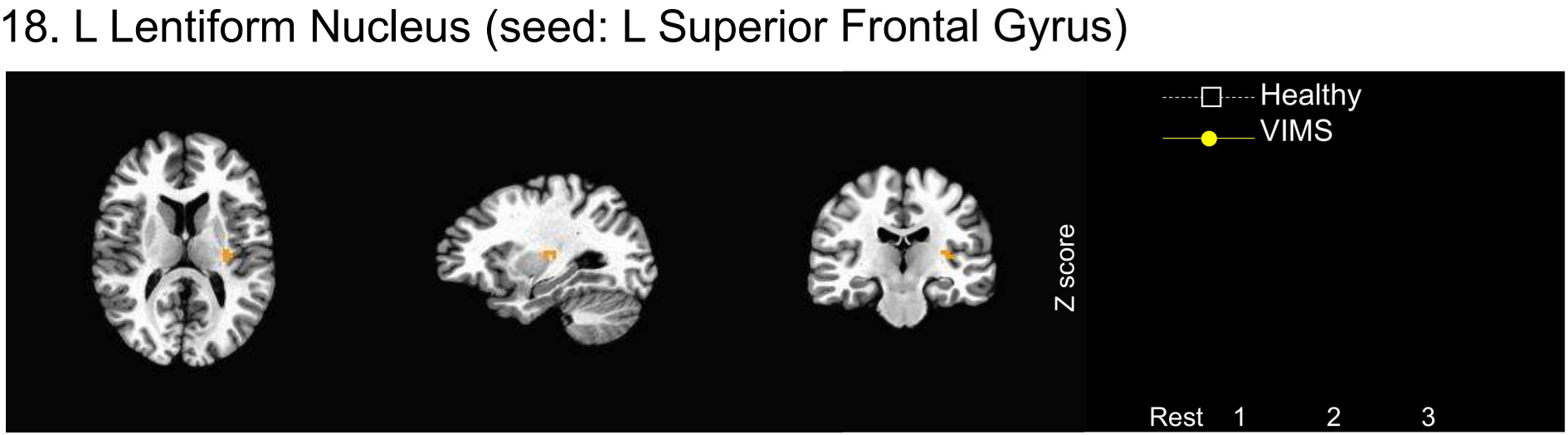

Figure 4. Brain regions whose functional connectivity with the seed regions increased in the recovery phase from visually induced motion sickness (VIMS)

The same as Figure 4a but for left lentiform nucleus.

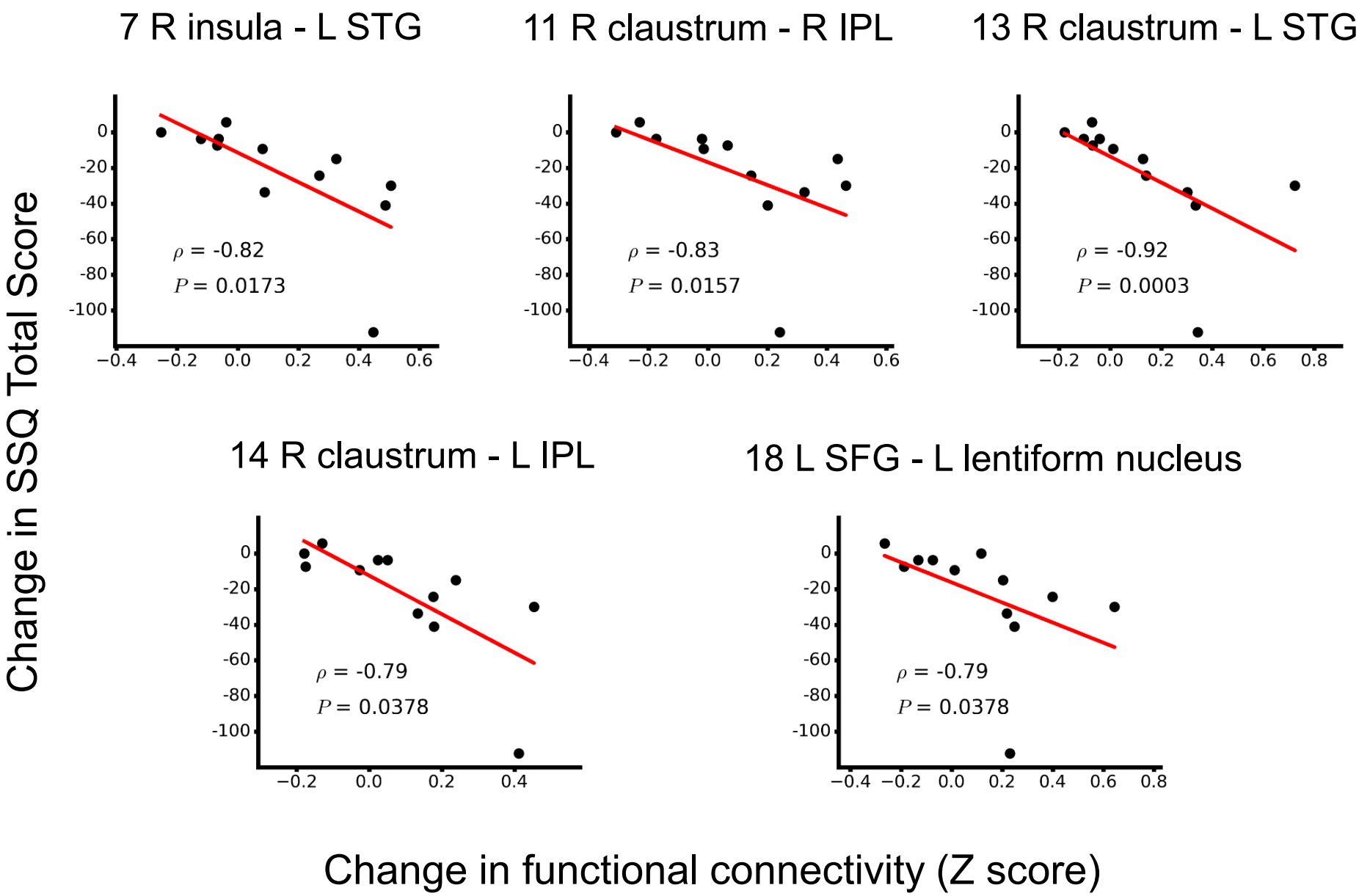

Figure 5. Correlation plots between the change in the Total Score (TS) of the Simulator Sickness Questionnaire (SSQ) and the change in functional connectivity

The vertical axis is the change in the TS of the SSQ: Rest-3 minus the average of Rest-1 and Rest-2; the more VIMS symptoms recovered, the more this score decreases. The horizontal axis is the change in functional connectivity: Rest-3 minus the average of Rest-1 and Rest-2. In the graphs, ρ indicates Spearman's rank correlation coefficient, with the corresponding *P* value shown below. The *P* values were Bonferroni corrected for multiple comparisons among the 19 brain region pairs. Abbreviations: IPL, inferior parietal lobule; L, left; R, right; SFG, superior frontal gyrus; STG, superior temporal gyrus.

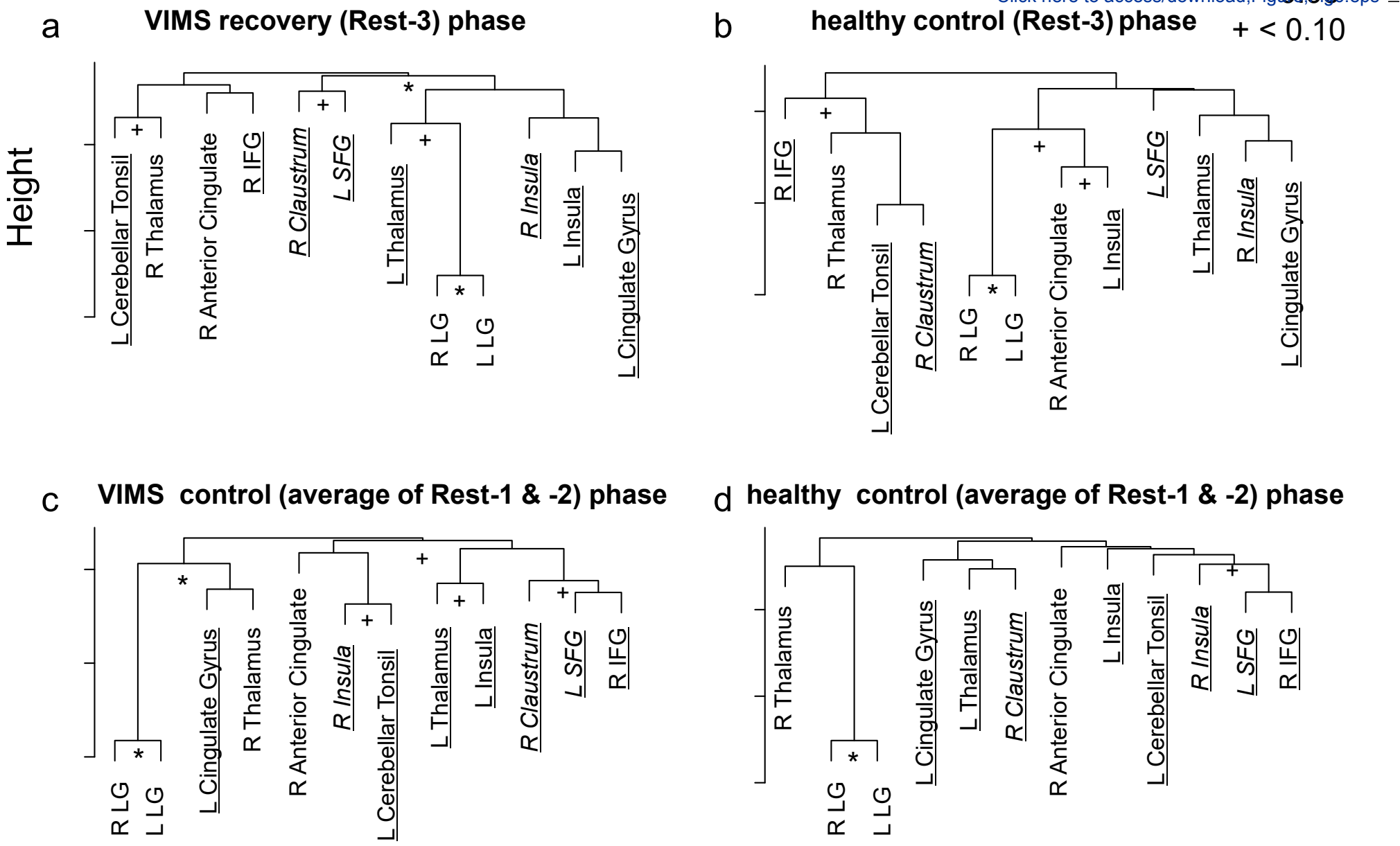

Figure 6. Hierarchical clustering trees of the 12 brain regions showing recovery-selective increases in connectedness

(a) The dendrogram of the VIMS group for the recovery phase (Rest-3), which was derived from the distance matrix (Supplementary Fig. 2a), whose elements indicate 1 minus absolute partial correlation between each pair of the 12 regions. Statistically significant clusters are marked with an asterisk ($P < 0.05$) or plus ($P < 0.1$). Brain regions showing recovery-selective increases in the ROI-based functional connectivity and correlations with SSQ are underlined and in italics, respectively. (b) The same as (a) but for the healthy group. (c) The same as (a) but for the control phase (the average of Rest-1 and Rest-2). (d) The same as (c) but for the healthy group. Abbreviations: L, left; R, right; LG, lingual gyrus; SFG, superior frontal gyrus; IFG, inferior frontal gyrus.

+Supplementary Materials

Resting-state functional connectivity predicts recovery from visually induced motion sickness

Jungo Miyazaki[1], Hiroki Yamamoto[2*], Yoshikatsu Ichimura[3], Hiroyuki Yamashiro[4], Tetsuya Yamamoto[5], Tomokazu Murase[6], Masahiro Umeda[7], Toshihiro Higuchi[6]

[1]Corporate R&D, Kyocera Corp., Kanagawa, Japan
[2]Graduate School of Human and Environmental Studies, Kyoto University, Kyoto, Japan
[3]Corporate R&D, Canon Inc., Tokyo, Japan
[4]Department of Medical Engineering, Aino University, Osaka, Japan
[5]Department of System Neuroscience, National Institute for Physiological Sciences, Aichi, Japan
Departments of [6]Neurosurgery and [7]Medical Informatics, Meiji University of Oriental Medicine, Kyoto, Japan

*Correspondence to: **Dr. Hiroki Yamamoto**
Graduate School of Human and Environmental Studies, Kyoto University
Yoshida Nihonmatsu-cho, Sakyo-ku, Kyoto 606-8501, Japan
E-mail: yamamoto@cv.jinkan.kyoto-u.ac.jp
Tel: +81-75-753-2978; Fax: +81-75-753-6574

Statistical assessment of the effects of head motion on functional connectivity

To clarify whether head motion affects functional connectivity, we statistically assessed the effect of head movement on functional connectivity. As a measure of head movement, the framewise displacement (FD) (Power et al. 2012) was computed. Then, the maximum value of FD during each rest phase was derived, and the effect of this maximum FD on the functional connectivity of 19 brain region pairs (listed in Tables 3–5) was tested with a linear mixed-effects model analysis. The linear mixed-effects model had fixed effects of the maximum FD (hereafter "FD") in addition to PHASE (Rest-1, -2, and -3) and GROUP (VIMS and healthy group) and three interactions of FD × PHASE, FD × GROUP, and PHASE × GROUP, as well as a random intercept for participants. A standard model selection technique was conducted using the *step* function in the lmerTest package (Kuznetsova *et al.* 2017) of R software. The *step* function statistically tests fixed effects based on the Satterthwaite method and removes ineffective terms from the model.

All 19 brain regions again showed a significant PHASE × GROUP interaction, confirming our results in the main text. The results for the effect of FD are shown in Supplementary Table 1, in which *P* values were not adjusted. For 15 brain region pairs among the 19 pairs, three head motion-related terms (that is the fixed effect of FD and the interactions of FD × PHASE and FD × GROUP) were not statistically significant, suggesting no effect of head motion on functional connectivity. A statistically significant FD × GROUP interaction was obtained for the remaining four pairs: the right claustrum–right inferior parietal lobule, right claustrum–left superior temporal gyrus, right claustrum–left inferior parietal lobule, and left superior frontal gyrus–left medial frontal gyrus. The PHASE × GROUP interaction was again statistically significant, even when the FD × GROUP interaction term and the simple effect of FD were included in the model as covariants. The *post hoc* interaction analyses essentially showed the same results for the VIMS group as those obtained with the original model without the covariants. For the healthy group, a slightly different result was obtained. There were simple effects of PHASE not found by the original model for two of the four pairs: the right claustrum–right inferior parietal lobule and the left superior frontal gyrus–left medial frontal gyrus. For these pairs, recovery-selective decreases in functional connectivity were shown for Rest-3 compared with Rest-2.

Extraction of independent brain networks with dictionary learning

To complement our main results, we performed a separate network analysis that extracted statistically independent resting networks related to the recovery from VIMS. A dictionary learning technique (Mensch et al. 2016) was applied for the fMRI data of the individuals in the VIMS group, using the *nilearn* module of Python (https://nilearn.github.io/). First, after preprocessing of the fMRI data as described in the main text, the data during the recovery phase were subjected to dictionary learning (*DictLearn* and *RegionExtractor* methods with the number of components = 15 and

minimum region size = 100 voxels), revealing 22 sparse regions of brain activities. Second, for each pair of the 22 brain regions, cross-correlation coefficients of fMRI time-series were computed, leading to a 22 × 22 matrix. Finally, this matrix was subjected to a connectome analysis using the *plot_connectome* function (edge threshold = 90%) in *nilearn*.

The result is shown in Supplementary Figure 3. Multiple brain regions critical for VIMS dynamics were found. The connectome map (Supplementary Figure 3b) shows visual processing regions, including the middle temporal gyrus and lingual gyrus, which were also found in the connectedness/functional connectivity approach used in the main text. These visual regions have been reported to have connectivity changes in the evolutional phase of VIMS (Miyazaki *et al.* 2015; Toschi *et al.* 2017). In addition, the cingulate region, which has been indicated to play key roles in the interoceptive process, such as self-awareness to one's own unpleasant bodily state, during/after VIMS, was detected in this analysis as well as that of the main text (Tables 2–5). Interestingly, the parahippocampal gyrus was again extracted in this analysis. The parahippocampal region is a core area for spatial memory processing (Epstein *et al.* 1998; Epstein, 2008), and memory processing has been suggested to be involved in an adaptation to motion sickness including VIMS (Reason & Brand 1975; Reason 1978; Oman 1990). This result thus suggests that such an adaptive process might underlie the recovery from VIMS. Altogether, this analysis corroborates our results reported in the main text.

References

Epstein, R. & Kanwisher, N. (1998) A cortical representation of the local visual environment. *Nature*, **392**, 598.

Epstein, R.A. (2008) Parahippocampal and retrosplenial contributions to human spatial navigation. *Trends in cognitive sciences*, **12**, 388-396.

Mensch, A., Mairal, J., Thirion, B. & Varoquaux, G. (Year) Dictionary learning for massive matrix factorization. City. p. 1737-1746.

Oman, C.M. (1990) Motion sickness: a synthesis and evaluation of the sensory conflict theory. *Canadian journal of physiology and pharmacology*, **68**, 294-303.

Power, J.D., Barnes, K.A., Snyder, A.Z., Schlaggar, B.L. & Petersen, S.E. (2012) Spurious but systematic correlations in functional connectivity MRI networks arise from subject motion. *Neuroimage*, **59**, 2142-2154.

Reason, J.T. (1978) Motion sickness adaptation: a neural mismatch model. *Journal of the Royal Society of Medicine*, **71**, 819-829.

Reason, J.T. & Brand, J.J. (1975) *Motion sickness*. Academic press.

Toschi, N., Kim, J., Sclocco, R., Duggento, A., Barbieri, R., Kuo, B. & Napadow, V. (2017) Motion sickness increases functional connectivity between visual motion and nausea-associated brain regions. *Autonomic Neuroscience*, **202**, 108-113.

Supplementary Table 1. Statistical analysis of the effect of head movement on functional connectivity

Seed region		Paired region	Hemispgere	Test statistics *P* value (*F* value)		
				FD	FD × GROUP	FD × PHASE
L Thalamus	1	Insula	Right	.739 (.113)	.501 (.722)	.578 (.318)
	2	Inferior Parietal Lobule	Right	.359 (.871)	.739 (.113)	.819 (.203)
	3	Declive	Right	.963 (.002)	.760 (.280)	.896 (.017)
L Insula	4	Thalamus	Left	.929 (.008)	.241 (1.44)	.888 (.120)
	5	Inferior Parietal Lobule	Right	.438 (.621)	.890 (.020)	.941 (.061)
R Insula	6	Thalamus	Left	.671 (.185)	.754 (.100)	.622 (.490)
	7	Superior Temporal Gyrus	Left	.459 (.563)	.191 (1.80)	.396 (.974)
	8	Inferior Temporal Gyrus	Left	.312 (1.06)	.082 (.3.26)	.661 (.424)
L Cerebellar Tonsil	9	Parahippocampal Gyrus	Left	.248 (1.40)	.086 (2.85)	.285 (1.19)
R Claustrum	10	Cingulate Gyrus	Left	.151 (2.19)	.362 (.860)	.624 (.485)
	11	Inferior Parietal Lobule	Right	-	.008 (8.22)	.596 (.533)
	12	Inferior Frontal Gyrus	Left	.633 (.233)	.162 (2.04)	.550 (.368)
	13	Superior Temporal Gyrus	Left	-	.030 (5.26)	.793 (.235)
	14	Inferior Parietal Lobule	Left	-	.046 (4.37)	.733 (.316)
L Cingulate Gyrus	15	Insula	Right	.542 (.381)	.671 (4.08)	.973 (.001)
L Superior Frontal Gyrus	16	Medial Frontal Gyrus	Left	-	.022 (6.11)	.367 (1.07)
	17	Middle Temporal Gyrus	Left	.88 (3.28)	.525 (.420)	.744 (.301)
	18	Lentiform Nucleus	Left	.130 (2.47)	.227 (1.54)	.518 (.683)
R Inferior Frontal Gyrus	19	Inferior Frontal Gyrus	Left	.485 (.502)	.364 (.857)	.418 (.921)

The effect of head motion (maximum framewise displacement [FD]) on functional connectivity was statistically assessed by using a linear mixed-effects model, in which a within-participants fixed effect of FD and interactions of FD × PHASE and FD × GROUP were included, in addition to the fixed effects of PHASE, GROUP, and PHASE × GROUP and a random effect of each individual participant. If the head movement-related interactions (i.e., FD × PHASE and FD × GROUP) were statistically significant, the statistics for FD were omitted because it was difficult to determine the effect.

a 1. R Insula (seed: R Thalamus)

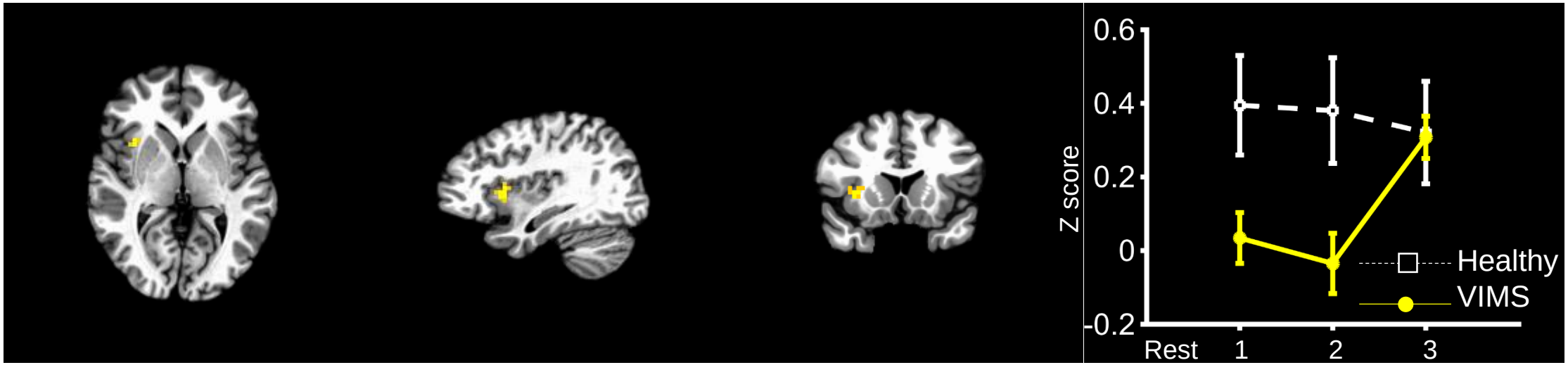

Supplementary Figure 1. Brain regions whose functional connectivity with the seed regions increased in the recovery phase from visually induced motion sickness (VIMS)

Each column shows, from left to right, axial, sagittal, and coronal brain images, and the change in functional connectivity (Z scores averaged within the participants' groups) of each experimental phase, separately for VIMS and healthy groups, respectively (error bars are standard errors). Each panel is the result for the following brain regions (the brain region in brackets is the corresponding seed): a–right insula (right thalamus), b–right inferior parietal lobule (right thalamus), c–right declive (right thalamus), d–left thalamus (left insula), e–right inferior parietal lobule (left insula), f–left thalamus (right insula), g–left inferior temporal gyrus (right insula), h–left parahippocampal gyrus (left cerebellar tonsil), i–left cingulate gyrus (right claustrum), j–left inferior frontal gyrus (right claustrum), k–right insula (left cingulate gyrus), l–left medial frontal gyrus (left superior frontal gyrus), m–left middle temporal gyrus (left superior frontal gyrus); and n–left inferior frontal gyrus (right inferior frontal gyrus). For this mapping, we used the following thresholds: voxel-wise threshold $P < 0.0001$, cluster level threshold $\alpha < 0.05$. The numbering of brain region pairs corresponds to that in Tables 3, 4, and 5.

b 2. R Inferior Parietal Lobule (seed: R Thalamus)

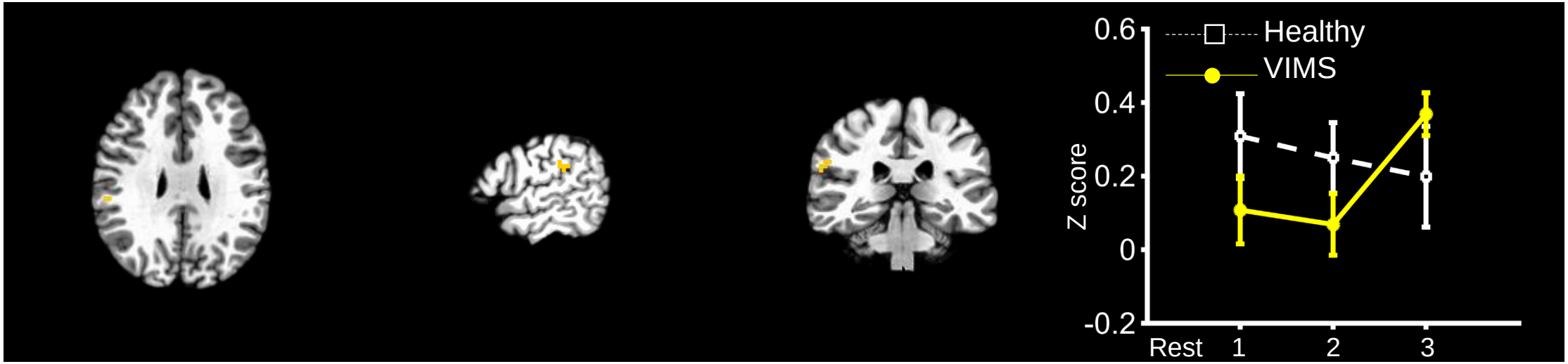

Supplementary Figure 1. Brain regions whose functional connectivity with the seed regions increased in the recovery phase from visually induced motion sickness (VIMS)

The same as Supplementary Figure 1a but for right inferior parietal lobule.

c 3. R Declive (seed: R Thalamus)

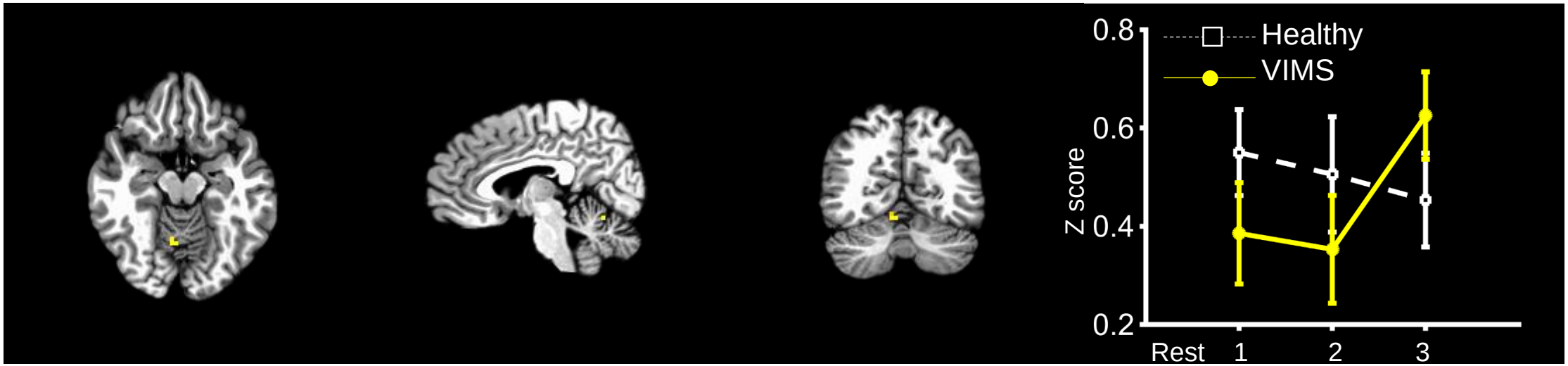

Supplementary Figure 1. Brain regions whose functional connectivity with the seed regions increased in the recovery phase from visually induced motion sickness (VIMS)

The same as Supplementary Figure 1a but for right declive.

d 4. L Thalamus (seed: L Insula)

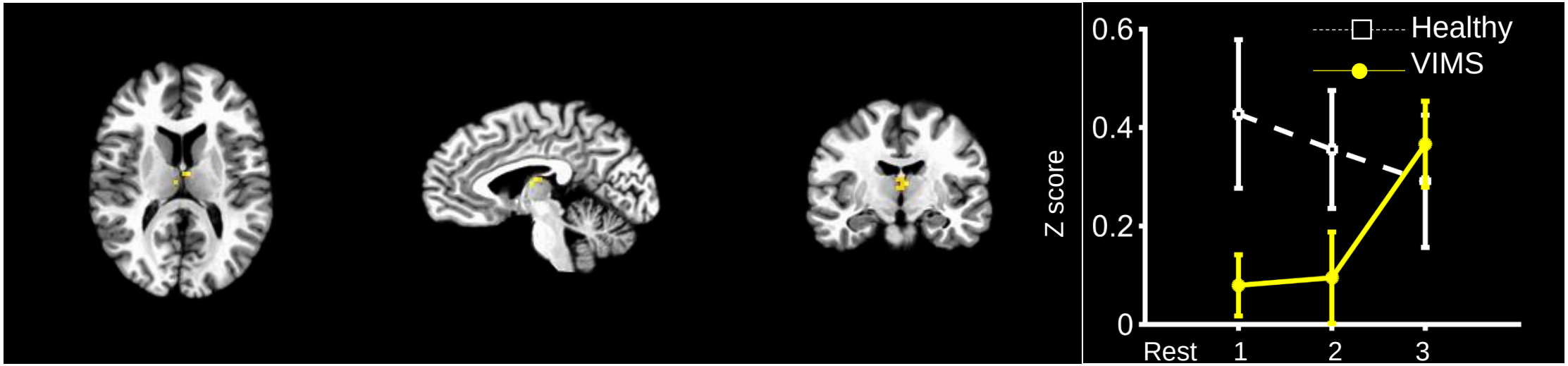

Supplementary Figure 1. Brain regions whose functional connectivity with the seed regions increased in the recovery phase from visually induced motion sickness (VIMS)

The same as Supplementary Figure 1a but for left thalamus.

e 5. R Inferior Parietal Lobule (seed: L Insula)

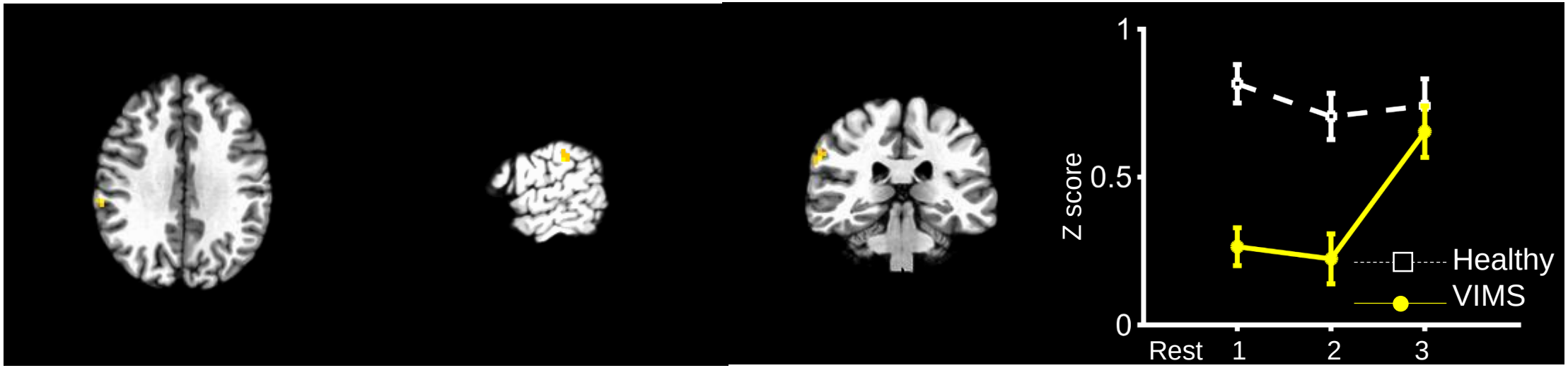

Supplementary Figure 1. Brain regions whose functional connectivity with the seed regions increased in the recovery phase from visually induced motion sickness (VIMS)
The same as Supplementary Figure 1a but for right inferior parietal lobule.

f 6. L Thalamus (seed: R Insula)

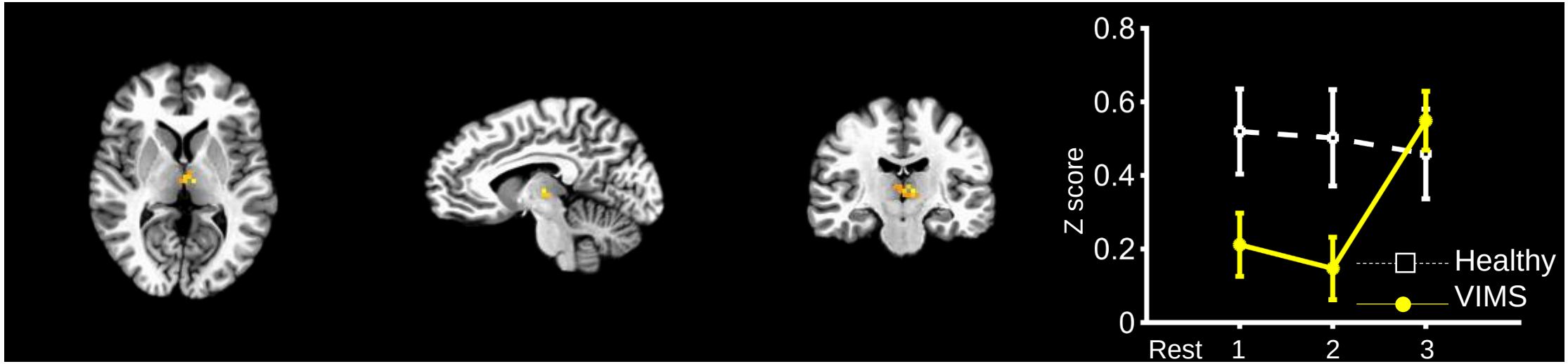

Supplementary Figure 1. Brain regions whose functional connectivity with the seed regions increased in the recovery phase from visually induced motion sickness (VIMS)

The same as Supplementary Figure 1a but for left thalamus.

g 8. L Inferior Temporal Gyrus (seed: R Insula)

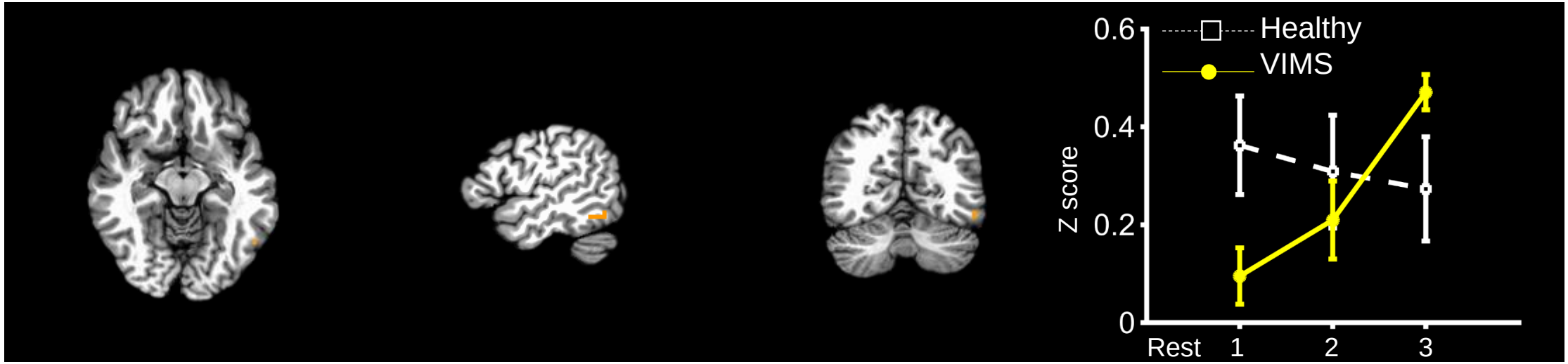

Supplementary Figure 1. Brain regions whose functional connectivity with the seed regions increased in the recovery phase from visually induced motion sickness (VIMS)

The same as Supplementary Figure 1a but for left inferior temporal gyrus.

h 9. L Parahippocampal Gyrus (seed: L Cerebellar Tonsil)

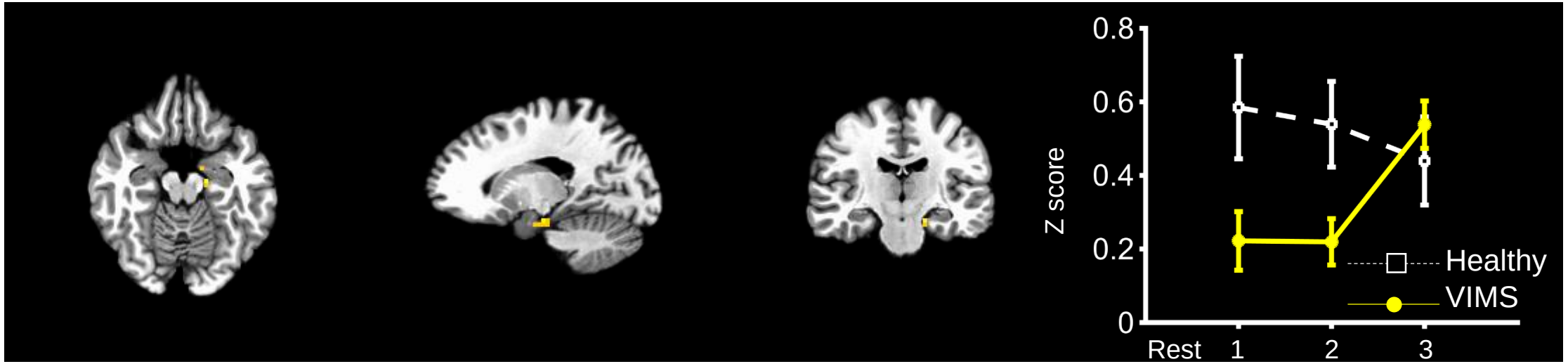

Supplementary Figure 1. Brain regions whose functional connectivity with the seed regions increased in the recovery phase from visually induced motion sickness (VIMS)

The same as Supplementary Figure 1a but for left parahippocampal gyrus.

i 10. L Cingulate Gyrus (seed: R Claustrum)

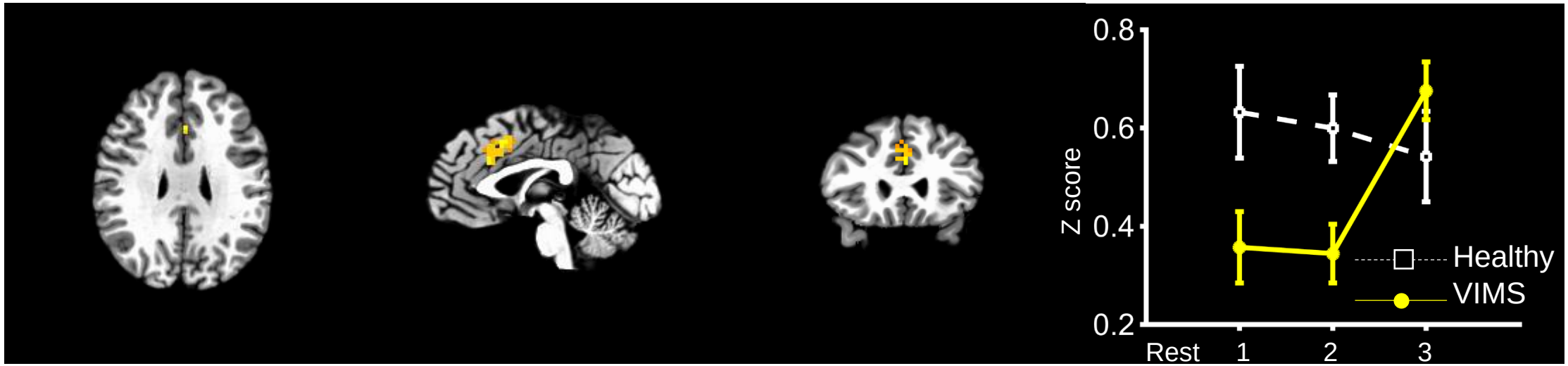

Supplementary Figure 1. Brain regions whose functional connectivity with the seed regions increased in the recovery phase from visually induced motion sickness (VIMS)
The same as Supplementary Figure 1a but for left cingulate gyrus.

j 12. L Inferior Frontal Gyrus (seed: R Claustrum)

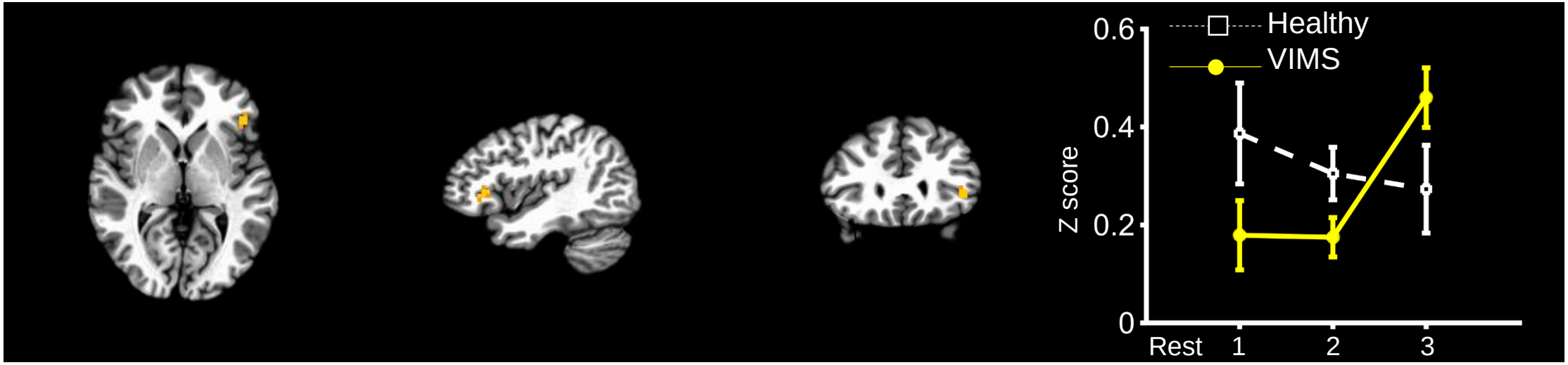

Supplementary Figure 1. Brain regions whose functional connectivity with the seed regions increased in the recovery phase from visually induced motion sickness (VIMS)

The same as Supplementary Figure 1a but for left inferior frontal gyrus.

k　15. R Insula (seed: L Cingulate Gyrus)

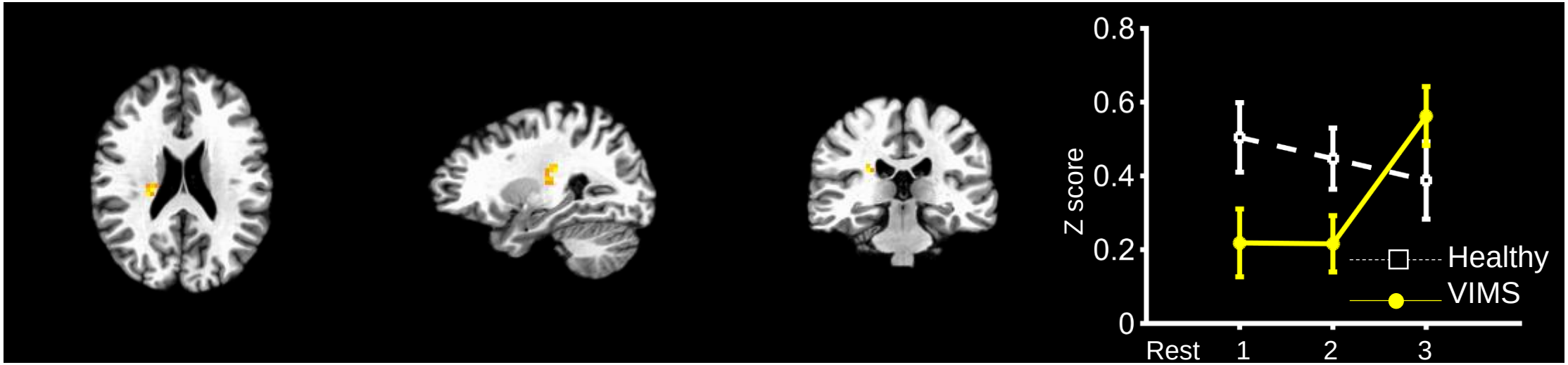

Supplementary Figure 1. Brain regions whose functional connectivity with the seed regions increased in the recovery phase from visually induced motion sickness (VIMS)
The same as Supplementary Figure 1a but for right insula.

l 16. L Medial Frontal Gyrus (seed: L Superior Frontal Gyrus)

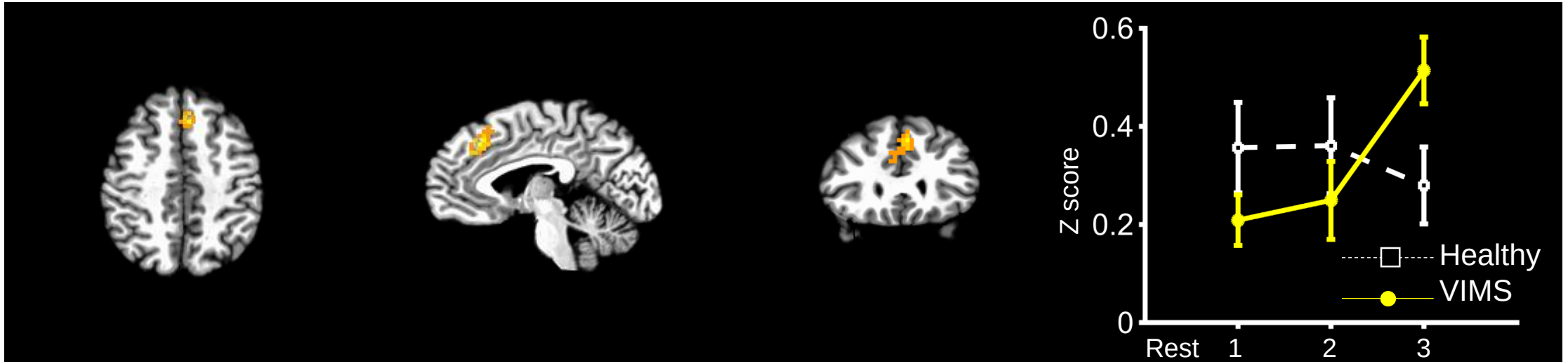

Supplementary Figure 1. Brain regions whose functional connectivity with the seed regions increased in the recovery phase from visually induced motion sickness (VIMS)

The same as Supplementary Figure 1a but for left medial frontal gyrus.

m　17. L Middle Temporal Gyrus (seed: L Superior Frontal Gyrus)

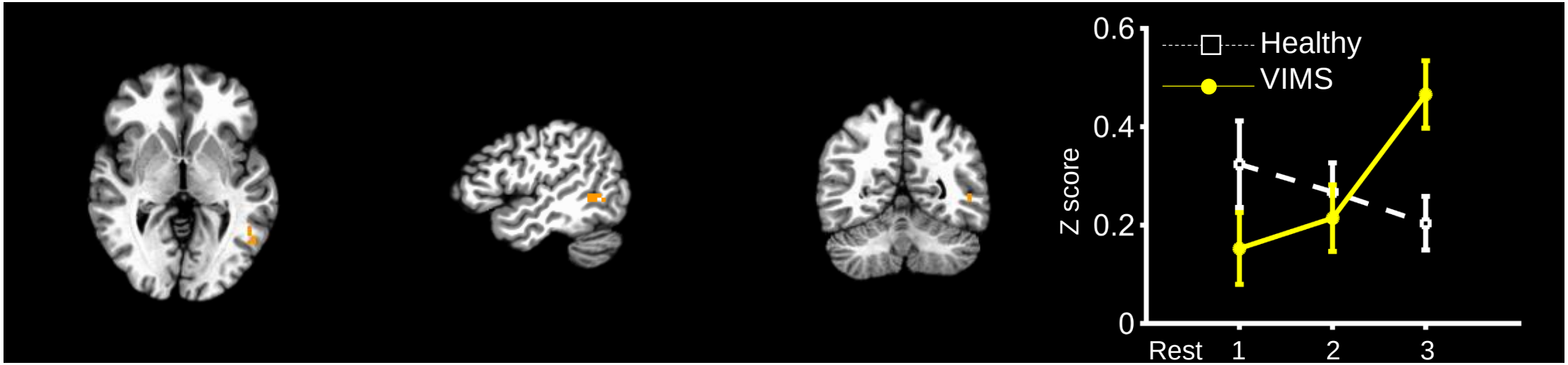

Supplementary Figure 1. Brain regions whose functional connectivity with the seed regions increased in the recovery phase from visually induced motion sickness (VIMS)
The same as Supplementary Figure 1a but for left middle temporal gyrus.

n 19. L Inferior Frontal Gyrus (seed: R Inferior Frontal Gyrus)

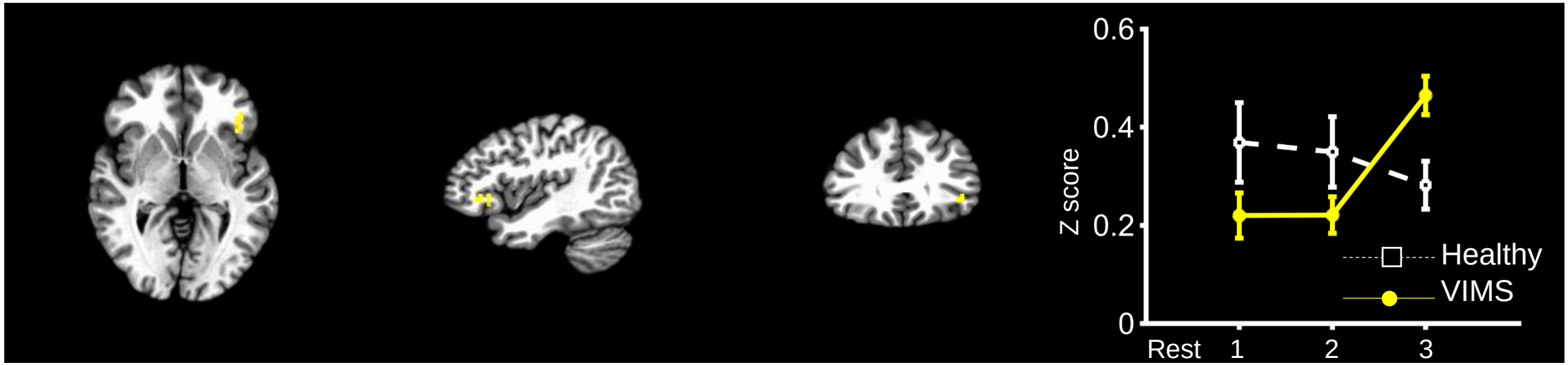

Supplementary Figure 1. Brain regions whose functional connectivity with the seed regions increased in the recovery phase from visually induced motion sickness (VIMS)
The same as Supplementary Figure 1a but for left inferior frontal gyrus.

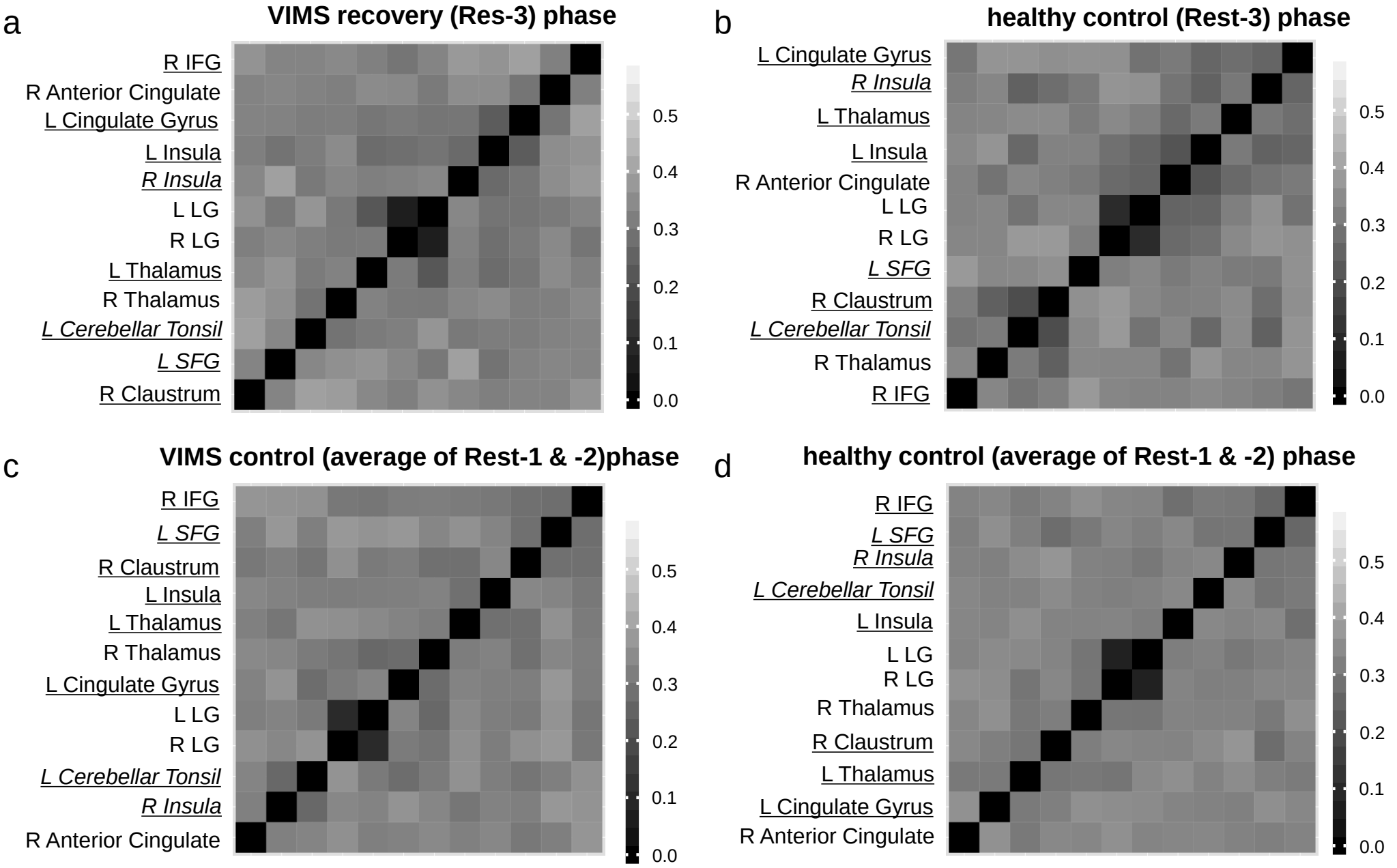

Supplementary Figure 2. Distance matrices of the 12 brain regions showing recovery-selective increases in connectedness

(a) The distance matrix of the VIMS group for the recovery phase (Rest-3), whose elements indicate 1 minus absolute partial correlation between each pair of the 12 regions. Brain regions showing recovery-selective increases in the ROI-based functional connectivity and correlations with SSQ are underlined and in italics, respectively. (b) The same as (a) but for the healthy group. (c) The same as (a) but for the control phase (the average of Rest-1 and Rest-2). (d) The same as (c) but for the healthy group. Abbreviations: L, left; R, right; LG, lingual gyrus; SFG, superior frontal gyrus; IFG, inferior frontal gyrus.

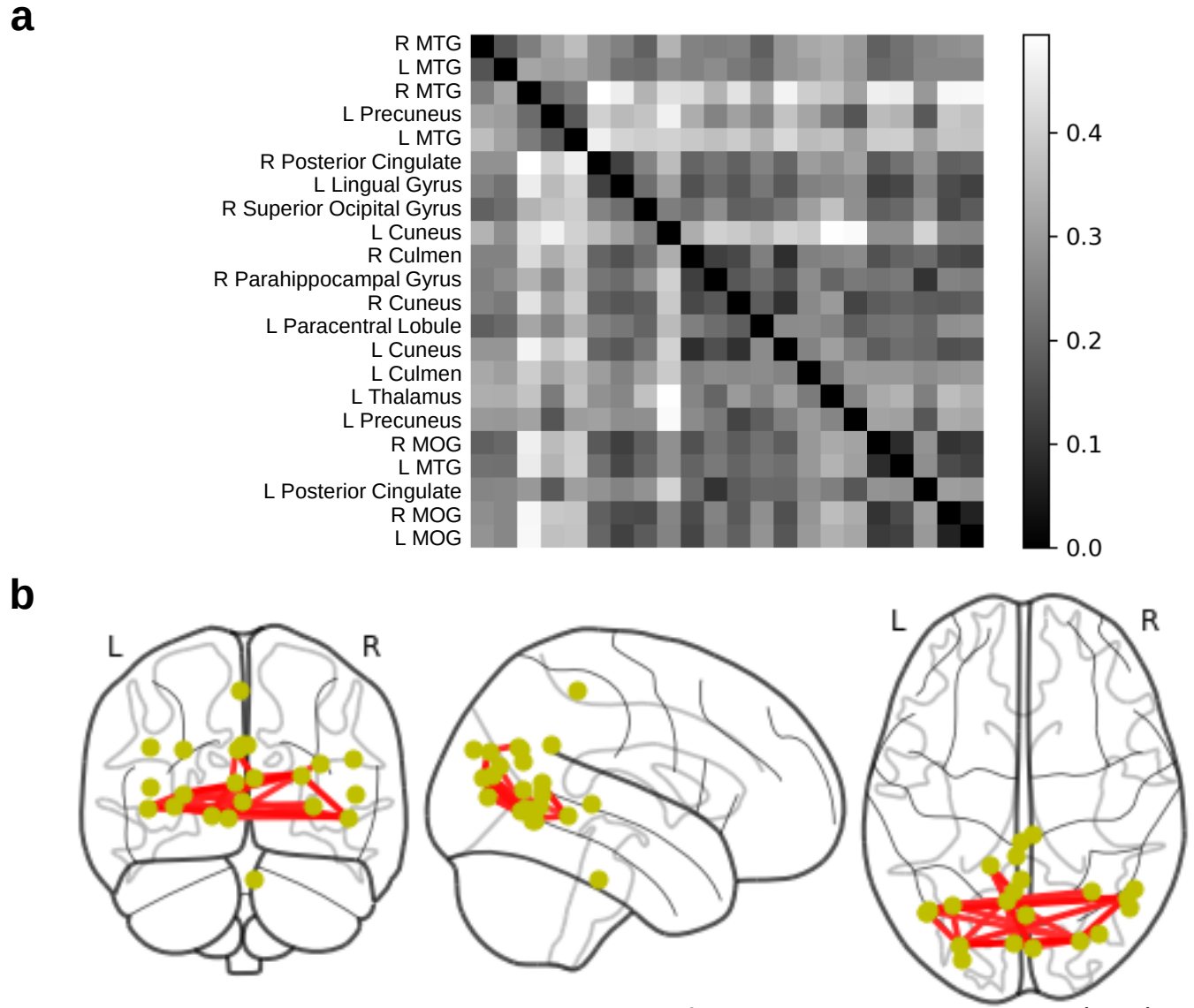

Supplementary Figure 3. Statistically independent brain networks related to recovery from visually induced motion sickness (VIMS)
(a) The within-participant averaged distance matrix for the recovery phase of the VIMS group. Each element represents a cross-correlation coefficient between each pair of the 22 regions determined by a dictionary learning technique. This analysis derived 22 regions of interest (ROIs). (b) The top 10% connections derived from the distance matrix. The connections are overlaid on a glass brain. Yellow circles and red lines denote the derived regions and connections, respectively. The connections are as follows: R Posterior Cingulate - L Lingual Gyrus, L Lingual Gyrus - R MOG, L Lingual Gyrus - L MTG, L Lingual Gyrus - R MOG, L Lingual Gyrus - L MOG, R Superior Ocipital Gyrus - R MOG, R Culmen - R Parahippocampal Gyrus, R Culmen - R Cuneus, R Culmen - L Cuneus, R Culmen - R MOG, R Culmen - L MOG, R Parahippocampal Gyrus - L Cuneus, R Parahippocampal Gyrus - L Posterior Cingulate, R Cuneus - L Cuneus, R Cuneus - L Precuneus, L Cuneus - R MOG, R MOG - L MTG, L MOG - R MOG, L MOG - R MOG, L MTG - R MOG, L MTG - L MOG, and R MOG - R MOG. Abbreviations: L, left; R, right; MTG, middle temporal gyrus; MOG, middle occipital gyrus.